We are IntechOpen,
the world's leading publisher of
Open Access books
Built by scientists, for scientists

6,900
Open access books available

185,000
International authors and editors

200M
Downloads

154
Countries delivered to

Our authors are among the

TOP 1%
most cited scientists

12.2%
Contributors from top 500 universities

CLARIVATE ANALYTICS
BOOK CITATION INDEX
INDEXED

WEB OF SCIENCE™

Selection of our books indexed in the Book Citation Index
in Web of Science™ Core Collection (BKCI)

Interested in publishing with us?
Contact book.department@intechopen.com

Numbers displayed above are based on latest data collected.
For more information visit www.intechopen.com

Novel Self-Oscillating Polymer Actuators for Soft Robot

Yusuke Hara, Shingo Maeda,Takashi Mikanohara, Hiroki Nakagawa, Satoshi Nakamaru and Shuji Hashimoto

Additional information is available at the end of the chapter

1. Introduction

Intelligent materials with changing properties and functions have been studied in many fields [1-9]. In particular, stimuli-responsive polymer systems have been considerably investigated for the purpose of the many types of possible applications, such as soft actuators, microfluidics and medical devices, *etc.* due to their light weight, flexibility and low noise, *etc.* [10-18]. Polymer gels have the flexible bodies allowing volume changes and sensors properties for chemical substances at the same time. By utilizing these properties, the gel actuators have been considered to be applied for the biomimetic robots. In particular, a thermoresponsive poly(N-isopropylacrylamide) (PNIPAAm) gel have been significantly investigated especially for medical devices. [19, 20] However, in order to drive these polymer materials, external device for controlling the external stimulus must be needed. On the other hand, organic systems can generate autonomous motion without external stimuli. In recent years, self-oscillating gels and polymer chains were developed and researched in order to understand and mimic the spontaneous mechanical works. [21-27] The energy source of self-oscillating polymer systems is chemical energy like a living organism, that is, the polymer system cause the self-oscillation induced by the Belouzov-Zhabotinsky (BZ) reaction or the pH oscillating reaction. [28-43] The Self-oscillating reactions have been widely studied for their relevance to nonlinear, chaotic dynamics and biological signals. In previous investigations, the self-oscillating behaviors of polymer systems induced by the Belousov-Zhabotinsky (BZ) or the pH oscillating reactions were realized.[44-60] The BZ reaction is well known as an oscillating reaction accompanying spontaneous redox oscillations to generate a wide variety of nonlinear phenomena, e.g., a target or spiral pattern in an unstirred solution, and periodicity, multi-periodicity, or chaos in a stirred solution. The overall process of the BZ reaction is the oxidation of an organic substrate by an oxidizing agent in the presence of the catalyst under strong acidic conditions. In the BZ

reaction, the metal catalyst undergoes spontaneous redox self-oscillation, and it changes the solubility from hydrophilic to hydrophobic at the same time. In order to cause the self-oscillation under temperature constant condition, the different solubility of the Ru catalyst in the reduced and oxidized state is utilized. In previous investigations, poly(Nisopropylacrylamide) (poly(NIPAAm)) was covalently bonded to (ruthenium (4-vinyl-4'-methyl-2,2-bipyridine) bis(2,2'-bipyridine)bis(hexafluorophosphate)) (Ru(bpy)₃) and a negatively charged acrylamide-2-methylpropanesulfonic acid (AMPS) as a pH and solubility control site [47-50]. The AMPS-containing polymer systems caused self-oscillations originating from the different solubility of the Ru(bpy)₃ moiety in the oxidized and reduced state. However, the conventional-type self-oscillating polymer system has the temperature limitation for causing the self-oscillation. That is because the conventional-type self-oscillating polymer system causes the aggregation or the contraction above the LCST. In this chapter, we introduce novel type self-oscillating polymers systems that are constituted the non-thermoresponsive and biocompatible poly-vinylpyrrolidone (PVP) as a polymer main-chain in order to expand the application fields. In our previous investigations, we first succeeded in causing the aggregation-disaggregation self-oscillation of the novel polymer chain and polymer gel under the constant condition induced by the BZ reaction. As for the VP-based self-oscillating polymer chain, the influence of the concentration of the three BZ substrates (sodium bromate, malonic acid and nitric acid) other than the metal catalyst on the waveform and period of the self-oscillation was investigated. As a result, it was demonstrated that the amplitude of the self-oscillation is hardly affected by the initial concentration of the BZ substrates. Furthermore, we firstly succeeded in causing the swelling-deswelling self-oscillation at high temperature condition by adapting the VP-main chain. We studied the influence of the initial concentration of the three BZ substrates other than the metal catalyst and the temperature on the period of the self-oscillation. As a result, it was clarified that the period of the self-oscillation for the VP-based polymer gel can be controllable by the selection of the initial concentration of the three BZ substrates (malonic acid (MA), sodium bromated (NaBrO₃) and nitric acid) and the temperature. In addition, by optimizing the initial concentration of the BZ substrates and the temperature, it was demonstrated that the maximam frequency of the swelling-deswlling self-oscillation is 0.5 Hz. This value was 20 times as large as that of the conventional-type self-oscillating polymer gel (poly(NIPAAm-co-Ru(bpy)₃ gel) with the thermoresponsive nature.

Next, in this chapter, we introduce the challenge of mimicking the peculiar locomotion of living organism, such as mollusks and apods, by utilizing polymer gel that cause the swelling-deswelling induced by the pH oscillating chemical reaction. Gastropods, like snails and slugs, can obtain the peristaltic movement by forming contraction waves, which is the propagation of the shrinking part of the body [61]. In this research, we focused on producing a functional gels obtaining peristaltic movements by the chemical energy directly.

In addition, we introduce a novel-tpye nanofiber gel actuator that was manufactured by the electrospining method. The nanofiber gel actuator can cause bending-streching motion

synchronized with the pH oscilltion. Polymer nanofibers have been much studied for the application to various fields, such as chemical detector, scaffolds, wound dressing, and multifunctional membranes, sensors, filtration media and biomaterials, *etc.* [62-65]. That is because the nanofiber gel membranes have a high surface-to-volume ratio and a relatively small pore size compared to normal-type polymer hydrogel. The merit of the electrospining method to manufacutre nanofiber gel actutors is low cost, relatively high production rate, and applicability to many types of polymers. Moreover, by utilizing the electrospinning method, we can construct various shapes of nanofiber gel actuators because it does not require a mold to synthesize the gel. By controlling the external conditions, we can construct more complex structures such as porous fiber, core sheathe fiber, *etc.* [66-69]. Recently, some researchers succeeded in manufacturing functional nanofiber gels by utilizing electrospining method. For example, Hsieh and coworkers have reported ultrafine gel fibrous membranes that consist of poly(acrylic acid) (PAAc), poly(N-isopropylacrylamide-*co*-acrylic acid) and poly(vinyl alcohol)(PVA) and PVA/PAAc mixtures [70-72]. However, there are a few challenges to realize the nanofiber gel actuator [73,74]. In this study, in order to construct an autonomous nanofiber gel actuator, we utilized Landolt pH-oscillator based on a bromated/ sulfite/ferrocyanide reaction. By coupling with this pH-oscillator, we realized a nanofiber gel actuator that shows the bending and stretching motions with a constant period and displacement.

2. Experimental section

2.1.1. Synthesis of the poly(VP-co-Ru(bpy)₃)

The polymer chain was prepared as follows. 0.5g of ruthenium(4-vinyl-4'-methyl-2,2'-bipylridine)bis(2,2'-bipyridine)bis(hexafluorophosphate) (Ru(bpy)₃) as a metal catalyst for the BZ reaction, 9.5 g of vinylpyrrolidone (VP) and 0.35 g of 2,2'-azobis(isobutyronitrile) (AIBN) as an initiator were dissolved in the methanol solution (31 g) under total monomer concentration of 20 wt%. These polymerizations were carried out at 60 °C for 24 h *in vacuo*. These resulting reaction mixtures were dialyzed against graded series of water/methanol mixtures, for 1 day each in 0, 25, 50, 75, and 100 wt% of water, and then freeze-dried.
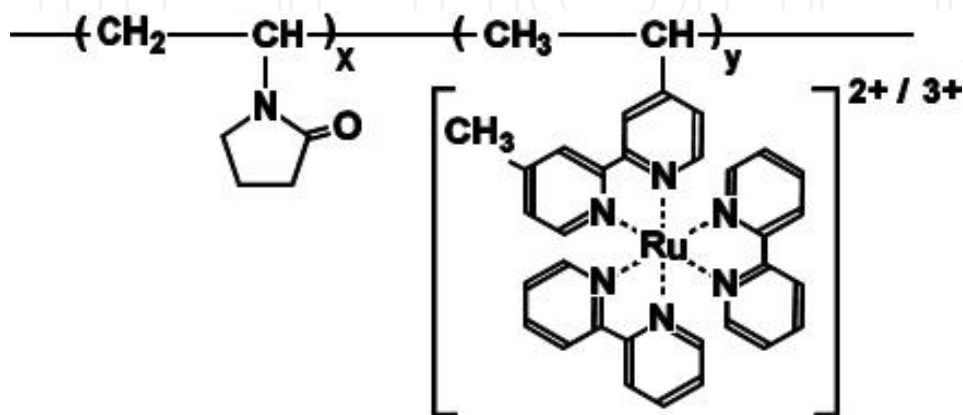

Figure 1. Chemical structure of poly(VP-*co*-Ru(bpy)₃).

2.1.2. Measurement of Lower Critical Solution Temperature (LCST) for the Poly(VP-co-Ru(bpy)₃) solution

The lower critical solution temperature (LCST) of the polymer solution was measured under the reduced and oxidized states, by using $Ce(SO_4)_2$ as an oxidizing agent and $Ce_2(SO_4)_3$ as a reducing agent, respectively. The polymer solutions (0.5 wt%) of poly(VP-*co*-Ru(bpy)₃) were prepared by dissolving the polymer in a 0.3 M HNO_3 aqueous solution and adding 5 mM $Ce(SO_4)_2$ or 5 mM $Ce_2(SO_4)_3$, respectively. The LCST measurements were carried out with a spectrophotometer (JASCO, Model V-630) equipped with magnetic stirrers and a thermostatic controller. In this measurement, the 570 nm wavelength was used because it is the isosbestic point for the reduced and oxidized states of Ru(bpy)₃. The transmittance (%) of the polymer solution at 570 nm was then recorded by raising the temperature at a rate of 0.5 °C/min.

2.1.3. Measurement of optical oscillations for the poly(VP-co-Ru(bpy)₃) solution

The poly(VP-*co*-Ru(bpy)₃) solutions were prepared by dissolving the polymer (0.5 wt%) into an aqueous solution containing the three BZ substrates (malonic acid (MA) and sodium bromate ($NaBrO_3$), nitric acid (HNO_3)). The transmittance self-oscillations of the polymer solutions were measured under constant temperature and stirring. In order to detect the transmittance change which is based on the autonomous transmittance change, 570-nm wavelength was used. The time course of the transmittance at 570 nm was monitored by a spectrophotometer.

2.2.1. Synthesis of the poly(VP-co-Ru(bpy)₃) gel

The gel was prepared as follows. 0.110g of Ru(bpy)₃ as a metal catalyst for the BZ reaction was dissolved in 0.877g of vinylpyrrolidone (VP). 0.012g of N,N'-methylenebisacrylamide (MBAAm) as a cross-linker, and 0.020g of 2,2'-azobis(isobutyronitrile) (AIBN) as an initiator were dissolved in the methanol solution (3ml) (Figure 1). The two solutions were mixed together well, and then the mixed solution purged with dry nitrogen gas. The monomer solution was injected between Teflon plates separated by silicone rubber as a spacer (thickness: 0.5mm), and then polymerized at 60°C for 18 hours. After gelation, the gel strip was soaked in pure methanol for a week to remove unreacted monomers. The gel was carefully hydrated through dipping it in a graded series of methanol-water mixtures, for 1 day each in 75, 50, 25 and 0%.

2.2.2. Measurements of the equilibrium swelling ratio of poly(VP-co-Ru(bpy)₃) gels

The equilibrium swelling ratio of the gels was measured under the reduced and the oxidized state, by using the oxidizing and the reducing agents. Gels were put into two solutions of Ce(III) and Ce(IV) under the same acidity, $[Ce_2(SO_4)_3]$=0.001M and $[HNO_3]$=0.3M; $[Ce_3(SO_4)_2]$=0.001M and $[HNO_3]$=0.3M, respectively. The equilibrium swelling ratio of the gels was observed and recorded by using a microscope (Fortissimo Corp.WAT-

250D), a LED light (LEDR-74/40 W), and a video recorder (Victor corp. SR-DVM700). The analysis was conducted by using the image processing software (Image J 1.38x). Measurements of the equilibrium swelling ratio were performed in a water-jacketed cell made of acrylic plates.
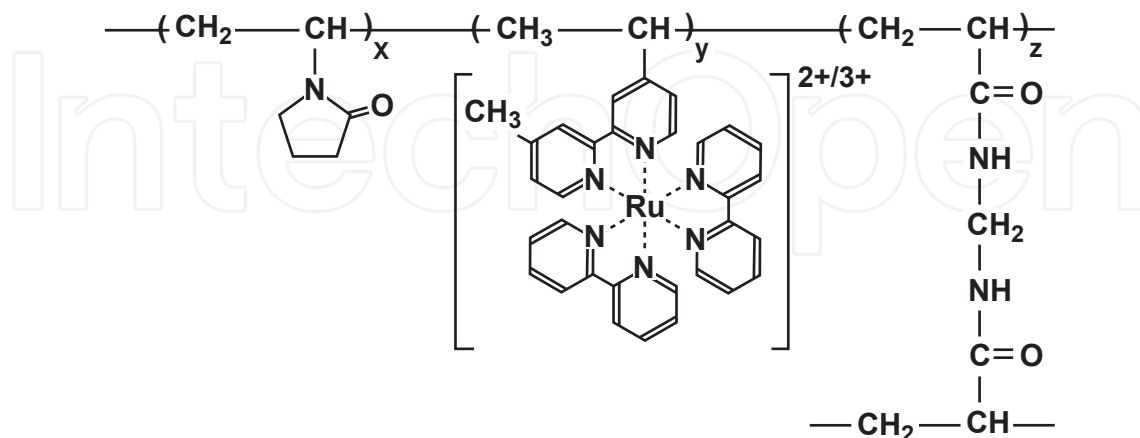
Figure 2. Chemical structure of poly(VP-co-Ru(bpy)₃) gel.

2.2.3. Measurements of the oscillating behavior for poly(Vp-co-Ru(bpy)₃) gels

The gel membrane was cut into rectangles(side length, about 2 × 20 mm) and immersed into 8mL of an aqueous solution containing malonic acid (MA), sodium bromate (NaBrO₃), and nitric acid (HNO₃). Shape changes of the gel strip were observed and recorded using a microscope (OLYMPUS.IX71), and a video recorder (Victor Corp. SR-DVM700). The analysis was conducted by using the image processing software (Image J 1.38x). A one-pixel line along the length of recorded gel image was stored at regular time intervals (0.05 s). The stored pixel line images were sequentially lined up as a function of time by the computer. This image processing procedure constructs a spatio-temporal diagram. From the obtained diagram, the time-dependent change in the gel edge was traced for observing the behavior of the volume change.

2.3.1. Synthesis of the poly(AAm-co-AAC) gel

The pH-responsive cylindrical hydrogels were prepared as follows. 0.533 g of acrylamide (AAm), 54.0 mg of acrylic acid (AAc), 12.8mg of N,N'-methylenebisacrylamide (MBAAm) as a cross-linker, and 22.6 mg of 2,2'-Azobis (2-methylpropionamidine) dihydrochloride as an initiator were dissolved in the O₂ free pure water (3.0 mL). The gelation was carried out in glass tubes (internal diameters from 1.0 mm to 2.0 mm) at 50 °C for 21 h. After removing from their molds, the cylindrical gels were cut in pieces 3.0 mm long and hydrated in pure water.

The pH-responsive cylindrical microphase-separated gels were prepared as follows. The composition of monomers is same as the cylindrical hydrogels, and they were dissolved in the solutions of O₂ free water/acetone mixtures (80/20, 70/30, 60/40, and 50/50 wt %). The polymerization was carried out in glass tubes (the size is same as above) at 50 °C for 21 h.

After removing from their molds, the cylindrical gels were also cut in pieces 3.0 mm long and hydrated in a graded series of methanol-water mixtures for 1 day each in 75, 50, 25, and 0 vol % methanol.

The pH-responsive microphase-separated tubular gel was prepared as follows. The composition of monomers is same as the cylindrical microphase-separated gels, and they were dissolved in the water/acetone mixture solution (70/30 wt %). The mold was made by coupling different size of glass tubes (external/internal diameters are 2.6/2.0, 1.0/0.6 mm), and the monomer solution was flowed into the tube-shaped space (external/internal diameters are 2.0/1.0 mm). The tubular gel was cut in pieces 4.0 cm long and hydrated in a graded series of methanol-water mixtures for 1 day each in 75, 50, 25, and 0 vol % methanol.

2.3.2. SEM Observation of the gels

Two samples were prepared in the following way. The microphase-separated gel cylinders were cut into pieces and soaked in acid (pH= 2) and base (pH = 11) solutions for 1 day until reaching the equilibrium. Then the gels were quickly frozen in liquid nitrogen and freeze-dried under vacuum for 1 day. The freeze-dried samples were fixed on the aluminum stubs and coated with the gold for 30 s under vacuum. The gel network structures were observed by the SEM (scanning electron microscope, HITACHI S2500CX).

2.3.3. Measurement of phase transition kinetics

In our measurement of the gels kinetics, two acid-base solutions with low and high pH (pH = 2 and pH = 11) were used. A piece of cylindrical gel under the equilibrium swelling in one solution was transferred quickly into the other. The changes of the cylindrical gel diameters were monitored by using a microscope equipped with a CCD camera controlled by a computer. The obtained images were analyzed by image processing software.

2.3.4. Experimental apparatus for causing the CT reaction in the pH-responsive tubular gel

The feeding solutions were stored in three separated reservoirs containing an alkaline sodium chlorite solution ($[NaClO_2] = 1.2 \times 10^{-1}$ M, $[NaOH] = 1.5 \times 10^{-4}$ M), an alkaline potassium tetrathionate solution ($[K_2S_4O_6] = 3.0 \times 10^{-2}$ M, $[NaOH] = 1.5 \times 10^{-4}$ M), and a sodium hydroxide solution ($[NaOH] = 1.3 \times 10^{-2}$ M). The solutions were pumped by peristaltic pumps (ATTO SJ-1211L) and premixed by a magnetic stirrer (AS-ONE CT-3A) before entering the tubular gel. The flows of chlorite and tetrathionate solutions were maintained at 30 mL/h, and the mixed solution flowed into the tubular gel by a peristaltic pump (ATTO SJ-1211H). The tubular gel was soaked in the mixed CT solution for 30 min in advance. After entering the flow of the mixed solution, an acid perturbation was applied by touching the gel at a particular spot with a paper soaked in a 1 M H_2SO_4 solution. The behavior of the tubular gel was observed by using a microscope equipped with a CCD camera controlled by a computer. Methyl red, a color indicator that changes from yellow

(basic) to red (acidic), was added to the solutions to directly visualize the propagation of acid regions. Fig. 3 shows the schematic illustration of experimental apparatus.
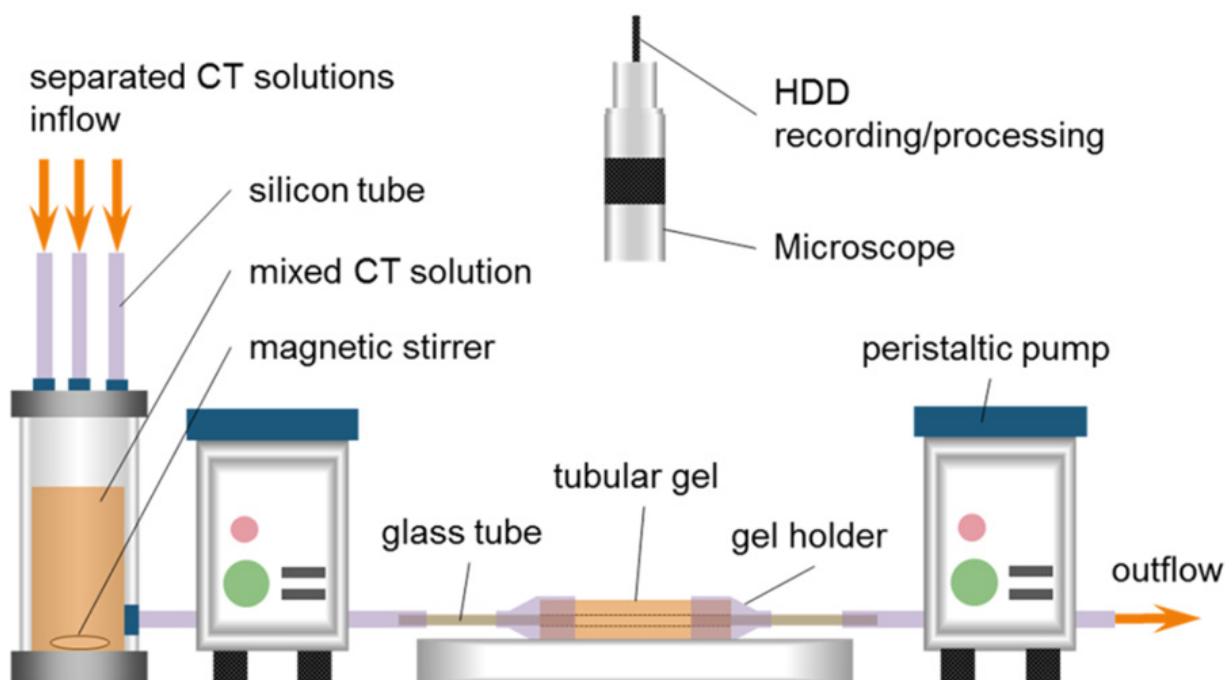

Figure 3. Schematic illustration of experimental apparatus for causing the CT reaction in the pH-responsive tubular gel. (Reprinted ref. 58, Copyright *IEEE*. Reproduced with permission.)

2.4.1. Preperation of Poly(AAc-co-tBMA)

Using AAc (25.9 g), tert- butyl methacrylate (tBMA) (34.1 g), and 2,2'-azobisiso-butyronitrile (AIBN) (0.49 g) as an initiator, *poly(AAc-co-tBMA)* (Figure 4) was synthesized by the radical polymerization in ethanol (139.5 g) using a total monomer concentration of 30 wt%. The molar ratio of tBMA incorporated into the copolymer was 30 mol%. The polymerization was carried out at 60 °C under nitrogen flow for 24 h. The resulting reaction mixture was dialyzed against ethanol for seven days.
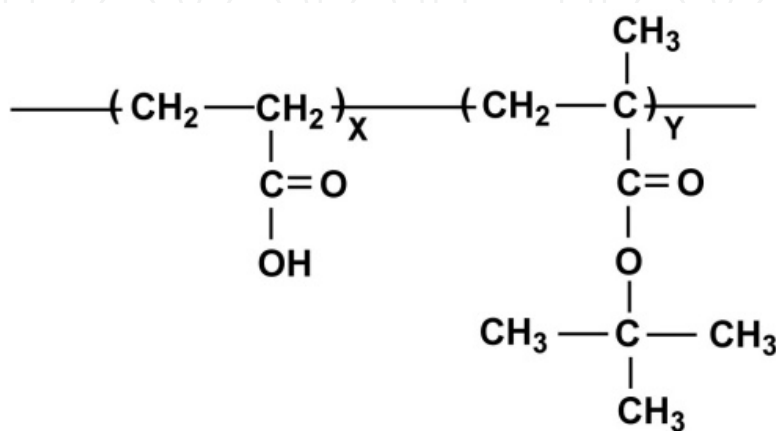

Figure 4. The chemical structure of poly(AAc-*co*-tBMA) polymer.

2.4.2. Electrospinning

The polymer solution (18 wt%) was poured into a 2.5 mL syringe. A potential of 10 kV was applied by connecting the power supply (GT80 GREEN TECHNO) to the syringe tip (Figure 5). In order to introduce anisotropic structure into the nanofiber gel, the 1.0 mL of the polymer solution in the syringe was sprayed at a flow rate of 2.0 mL/hour (sprayed for 30 minutes), and then the flow rate was changed to 1.0 mL/hour (sprayed for 60 minutes). The fibers were collected on the grounded glass substrate as a collector. The distance between the collector and the syringe tip was 15 cm. The temperature and humidity were 25 °C and 70%, respectively. After the electrospinning, the obtained sheet, with a thickness of about 200 μm, was dried overnight at 50 °C.
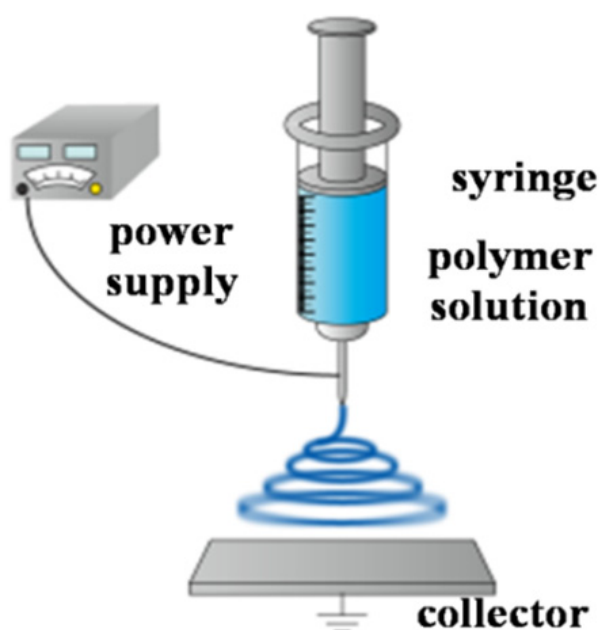

Figure 5. Schematic illustration of electrospinning set-up.

2.4.2. Measurement of motion of the nanofiber gel actuator

The open continuously stirred tank reactor (CSTR) (40 mL) was designed using an acrylic cell with a water jacket in order to control the solution temperature in the cell. Potassium bromated (0.26 mol/L), sodium sulfite (0.3 mol/L), potassium ferrocyanide (0.08 mol/L), and sulfuric acid (0.04 mol/L), solutions were pumped into the reactor at a flow rate of 50 mL/hour. The pH changes in the reactor were monitored continuously by utilizing a pH meter (F-55 HORIBA) held in the reactor, and its electronic output was directly recorded by a computer. The nanofiber gel (length 15 mm, width 3 mm) was set at the bottom of the water jacket. One end of the gel strip was sandwiched in the incision of the silicone rubber. Shape changes of the gel strip were recorded by a fixed microscope (Fortissimo Corp. WAT-250D) and a video recorder (Victor Corp. SR-DVM700). The temperature in the reactor was controlled at 25 °C by utilizing the water bath equipment.

3. Results and discussion

3.1. Self-oscillating behavior of poly(VP-*co*-Ru(bpy)$_3$) solution

The measurement of the solubility for the poly(VP-*co*-Ru(bpy)$_3$) solution in the reduced and oxidized state was conducted by changing the temperature from 10 to 50 °C. As shown in Figure 6, there are no the lower critical solution temperature (LCST) for the polymer solutions in the reduced and oxidized state. The polymer solutions in the reduced and oxidized state have different transmittance values. That is, this result indicates that the polymer solution has different solubility in the reduced and oxidized state, respectively. The solubility of the polymer solution in the reduced state is higher than that in the oxidized state. Figure 7 shows self-oscillating behaviors of the poly(VP-*co*-Ru(bpy)$_3$) solution in the different concentrations of malonic acid ([MA] = 0.04, 0.05, 0.06, 0.07, 0.08 and 0.09 M) under the fixed concentration of sodium bromate and nitric acid ([NaBrO$_3$] = 0.3 M and [HNO$_3$] = 0.3 M). As shown in Figure 7, the base line of the transmittance self-oscillation gradually decreased with time in all malonic acid concentrations. The damping behavior originates from the change in the ionic strength of the polymer solution when the transmittance measurement starts [47-49]. In order to cause the BZ reaction in the polymer solution, the self-oscillating polymer solution and the other solution of the BZ substrates are mixed just before the transmittance measurements. In general, the solubility of the polymer chain is significantly affected by the ionic strength of the solution. Therefore, when the ionic strength increased at the start point of the self-oscillation, the solubility of the polymer chain decreased. In the solution condition of this study, the ionic strength of the polymer solution was very high because the BZ reaction required a significant high concentration of the BZ substrates. Therefore, the damping behaviors occurred from the start point of the self-oscillation. In addition, as shown in Figure 7, the width of the waveform increased with decreasing the concentration of malonic acid. Basically, the width of the waveform of the transmittance self-oscillation depends on the rate of the BZ reaction because the self-oscillation was induced by the BZ reaction. As the concentration of the BZ substrates decreased, the rate of the BZ reaction decreased due to decrease in the collision rate among the BZ substrates. Therefore, the width of the waveform increased with decreasing concentration of the BZ substrates. This tendency was observed in the transmittance self-oscillation of the AMPS-containing polymer solutions [48].

Figure 8 shows the transmittance self-oscillations of the novel polymer solution in the different concentration of sodium bromate ([NaBrO$_3$] = 0.1, 0.2, 0.3 and 0.4 M) at 14 °C under the fixed concentration of malonic acid and nitric acid ([MA] = 0.1M and [HNO$_3$] = 0.3 M). As shown in Figure 8, the amplitude of the self-oscillation gradually decreased with time in the same manner as in Figure 7. Moreover, the width of the waveform decreased with the increase in the concentration of sodium bromate due to the increase in the reaction rate of the BZ reaction. In addition, as shown in Figure 8, the amplitudes of the transmittance self-oscillations were hardly affected by the initial concentration of sodium bromate. In additon, Figure 9 showed the amplitude of the transmittance self-oscillation for the polymer solution under the different concentrations of the BZ substrates. As shown in Figure 9, all the BZ

substrate concentrations hardly influence the amplitude of the transmittance self-oscillation. That is, the amplitude values were almost the same in all BZ substrate conditions. In our previous investigations, we studied the effect of the concentration of the BZ substrates on the waveform of the transmittance self-oscillation for the AMPS-containing polymer solution. As a result, we clarified that the amplitude of the self-oscillation is significantly affected by the initial concentration of the BZ substrates [47-49]. This is because the AMPS-containing polymer chain caused damping, that is, the amplitude of the self-oscillation gradually decreased with time. The damping behavior of the polymer solution originates from the change in the size of the polymer aggregation with time. In the case of the NIPAAm-based polymer chains, the reduced Ru moiety in the polymer chain strongly interacts with the other reduced Ru one. Once the reduced Ru moiety strongly interacts with the other Ru one, the interaction hardly dissociates [48]. In the BZ reaction, the time in the reduced state is much longer than in the oxidized state. Therefore, the hydrophobic $Ru(bpy)_3^{2+}$ moiety in the polymer chain dominantly behaved for the determination of the polymer aggregation state in the self-oscillating behavior. For this reason, the mole fraction of the $Ru(bpy)_3^{2+}$ moiety in the polymer chain significantly affect the waveform of the transmittance self-oscillation. This influence can be explained by the overall process of the BZ reaction based on the Field-koros-Noyes (FKN) mechanism [33-36, 48]. On the other hand, in the case of the VP-based polymer chain, the bipyridine ligands interacted with the VP based main-chain. The strength of the interaction of the bipyridine ligands in the oxidized state is higher than in the reduced state. That is, the polymer aggregation increased in the oxidized state. However, the time in the oxidized state is much shorter than in the reduced state. Therefore, the size of the polymer aggregation changed very slowly compared to the AMPS-containing polymer solution. Consequently, the degree of the damping for the Vp-based polymer solution is considerably small. Therefore, the amplitude is hardly affected by the initial concentration of the BZ substrates.
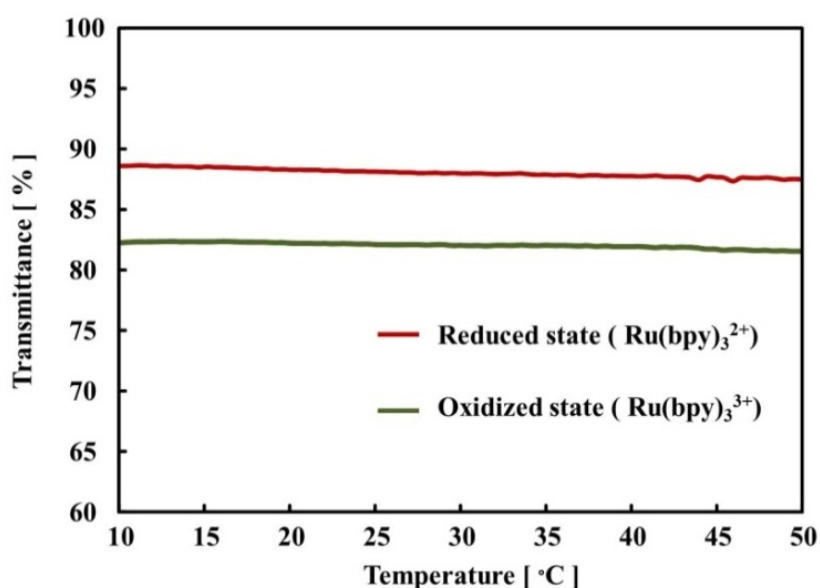

Figure 6. Temperature dependence of transmittance for poly(VP-*co*-Ru(bpy)₃) solutions under the different conditions of reduced Ru(II) (in Ce(III) solution) and Ru(III) (in Ce(IV) solution) states.
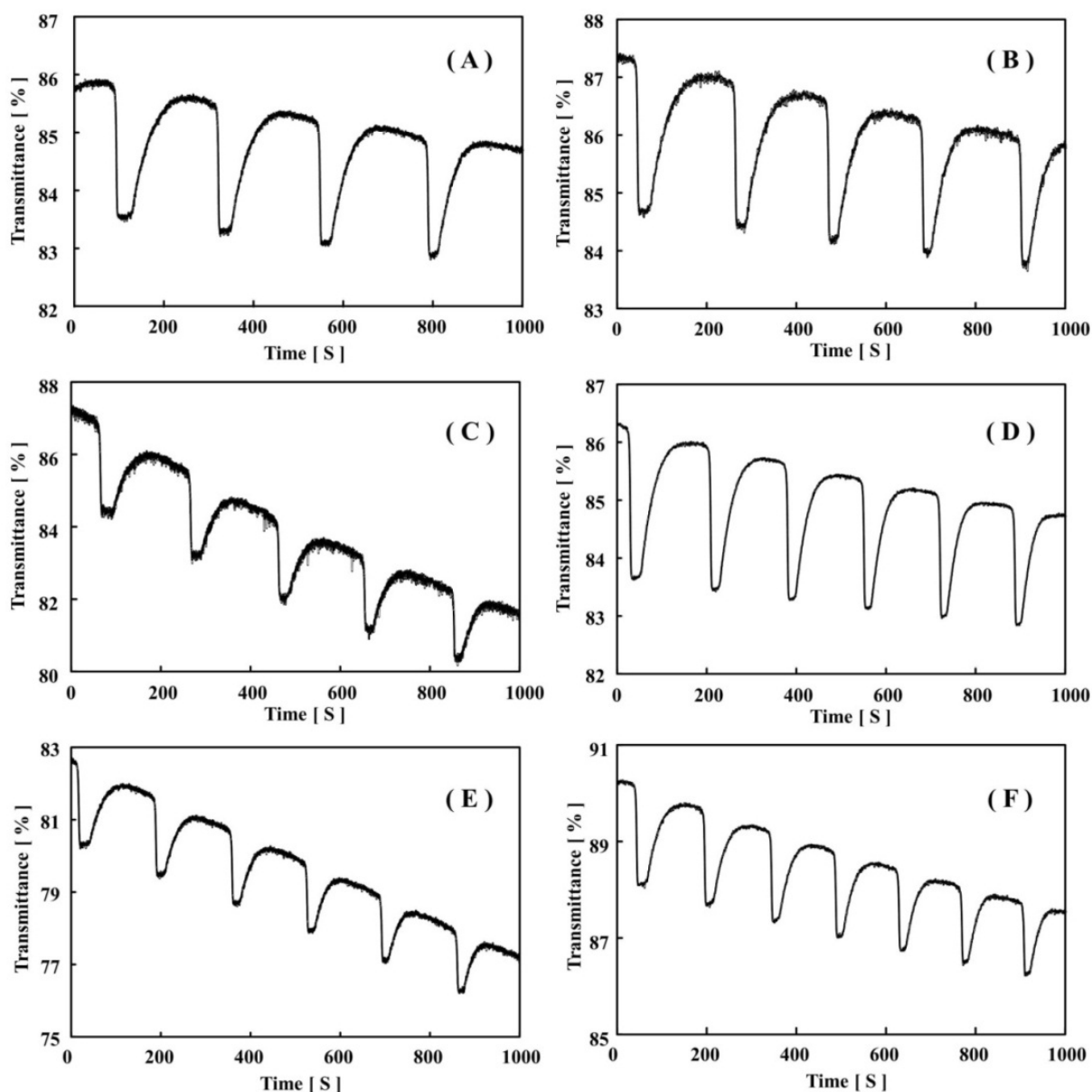
Figure 7. Oscillating profiles of transmittance at 14 °C for 0.5 wt% poly(VP-*co*-Ru(bpy)₃) solution in the fixed nitric acid and sodium bromate conditions ([HNO₃] = 0.3 M and [NaBrO₃] = 0.3 M): (**A**) [MA] = 0.04 M, (**B**) [MA] = 0.05 M, (**C**) [MA] = 0.06 M, (**D**) [MA] = 0.07 M, (**E**) [MA] = 0.08 M, (**F**) [MA] = 0.09 M.

3.2. Self-oscillating behavior of poly(VP-*co*-Ru(bpy)₃) gel

Figure 10 shows the equilibrium swelling behaviors of the poly(VP-*co*-Ru(bpy)₃) gels in the Ce(III) and Ce(IV) solutions under the same acidic condition. In the Ce(III) solution, the gel kept a tinge of orange, which indicated that the copolymerized Ru(bpy)₃ moiety in the gel was in the reduced state. On the other hand, in the Ce(IV) solution, the gel quickly turned from orange to green, which showed the Ru(bpy)₃ moiety in the gel had changed the reduced state to the oxidized state. In the oxidized state, the equilibrium volume of the gel was larger than that in the reduced state in all temperature condition. This is because the solubility of the Ru(bpy)₃ moiety has significantly different properties in the oxidized and
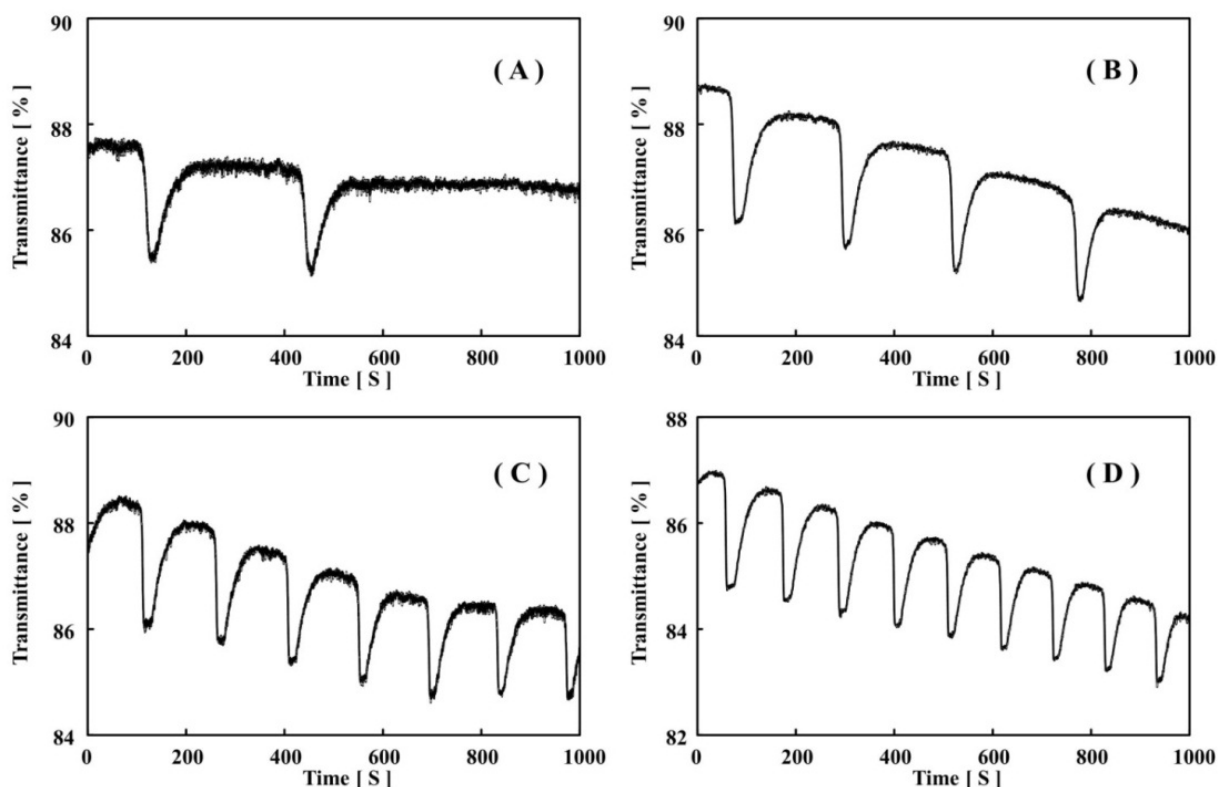
Figure 8. Oscillating profiles of transmittance at 14 °C for 0.5 wt% poly(VP-*co*-Ru(bpy)₃) solution in fixed nitric acid and malonic acid conditions ([HNO₃] = 0.3 M, [MA] = 0.1 M) (**A**) [NaBrO₃] = 0.1 M, (**B**) [NaBrO₃] = 0.2 M, (**C**) [NaBrO₃] = 0.3 M, (**D**) [NaBrO₃] = 0.4 M.
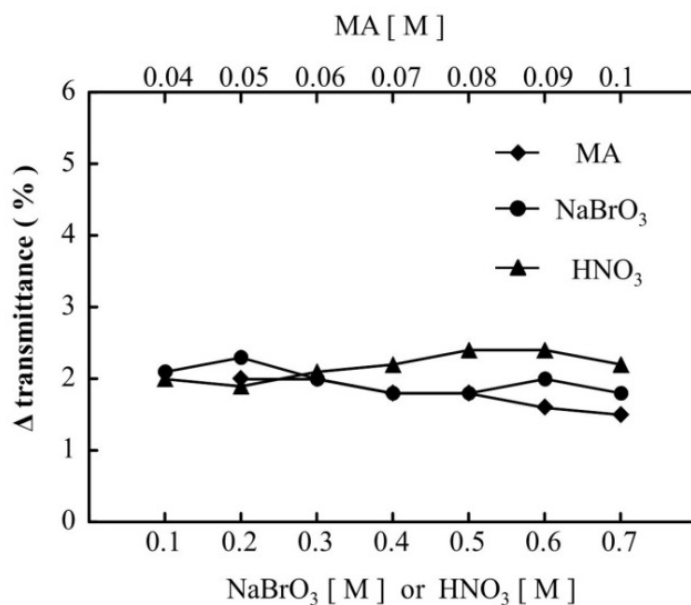

Figure 9. Dependence of amplitude of transmittance self-oscillation for polymer solution at 14 °C in the change in one BZ substrate under fixed concentrations of the other two BZ substrates: **MA** ([MA] = 0.04, 0.05, 0.06, 0.07, 0.08 and 0.09 M, fixed [NaBrO₃] = 0.3 M and [HNO₃] = 0.3 M); **NaBrO₃** ([NaBrO₃] = 0.1, 0.2, 0.3, 0.4, 0.5 and 0.6 M, fixed [MA] = 0.1 M and [HNO₃] = 0.3 M); **HNO₃** ([HNO₃] = 0.1, 0.2, 0.3, 0.4, 0.5 and 0.6 M, fixed [NaBrO₃] = 0.1 M and [HNO₃] = 0.3 M).

reduced state. The reduced Ru(bpy)₃ moiety in the gel has an extreme hydrophobic property in the VP-based polymer gel. This property is attributed to the conformation of the bipyridine ligands surrounding the Ru ion, which induces the deswelling behavior. That is, in the VP-based gel, the bipyridine ligands surrounding the Ru ion exert a greater influence on the solubility of the polymer chain in the reduced state as compared with the ionization effect of the Ru ion.[47-52] On the contrary, the oxidized Ru(bpy)₃ parts in the gel has a great hydrophilic property. The driving force of the swelling-deswelling self-oscillation is originated in the different solubility of the Ru(bpy)₃ moiety in the reduced and oxidized states as shown in Figure 10. In the reduced and oxidized state, there is no observation of the volume phase transition because of the PVP main chain of the gel without LCST.
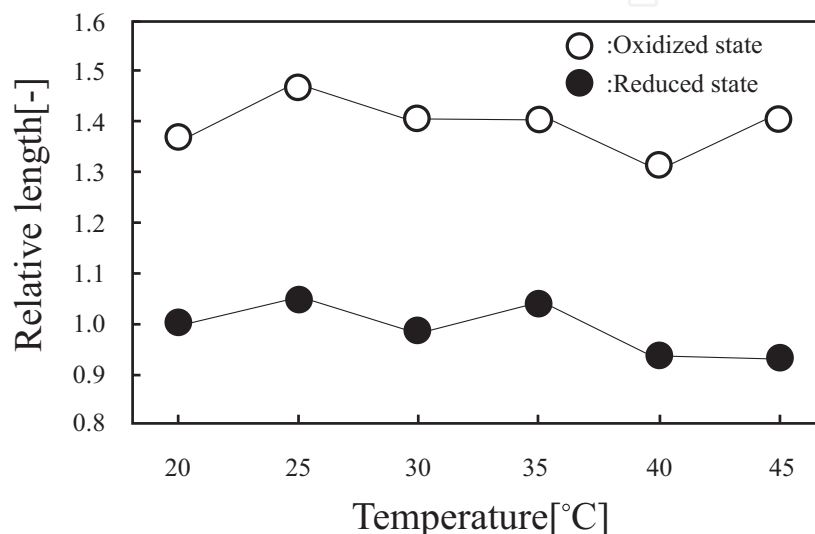

Figure 10. Equilibrium swelling ratio of poly(VP-*co*-Ru(bpy)₃) gel in cerium sulfate solutions as a function of temperature. (●) [Ce₂(SO₄)₃] = 0.001M and [HNO₃] = 0.3M; (○) [Ce(SO₄)₂] = 0.001M and [HNO₃] = 0.3M. The relative length is defined as the ratio of characteristic diameter at the initial state at 20°C. (Reprinted ref. 57, Copyright American Chemical Society. Reproduced with permission.)

Figure 11 showed the logarithmic plots of the period against the initial concentration of one BZ substrate under fixed concentration of the other two BZ substrates at a constant temperature (*T*=20 °C). As shown in Figure 11, all the logarithmic plots had a good linear relationship. Therefore, the period [T(s)] of the swelling-deswelling self-oscillation can be expressed as *a*[substrate]*ᵇ* where *a* and *b* are the experimental constants, and the brackets indicate the initial concentration. Moreover, as shown in Figure 11, the period of the self-oscillation have the saturation point at the following initial concentration: [MA] = 0.07M (Figure 11(a)), [NaBrO₃] = 0.5M (Figure 11(b)) and [HNO₃] = 0.7M (Figure 11(c)). The period at the saturated point in Figure 11(a) was significantly higher than that in Figure 11(b) and Figure 11(c). This tendency can be explained by considering the mole fraction of the reduced Ru(bpy)₃ moiety in the gel. This is because the reduced Ru(bpy)₃ moiety in the gel has the significantly high hydrophobic property. Therefore, the number of the hydrophobic reduced Ru(bpy)₃ moiety in the gel exert influence of the self-oscillating behavior. The Field-koros-Noyes (FKN) mechanism explained the overall process of the BZ reaction. [33-36, 48] According to the FKN mechanism, the overall reaction is divided into the following three
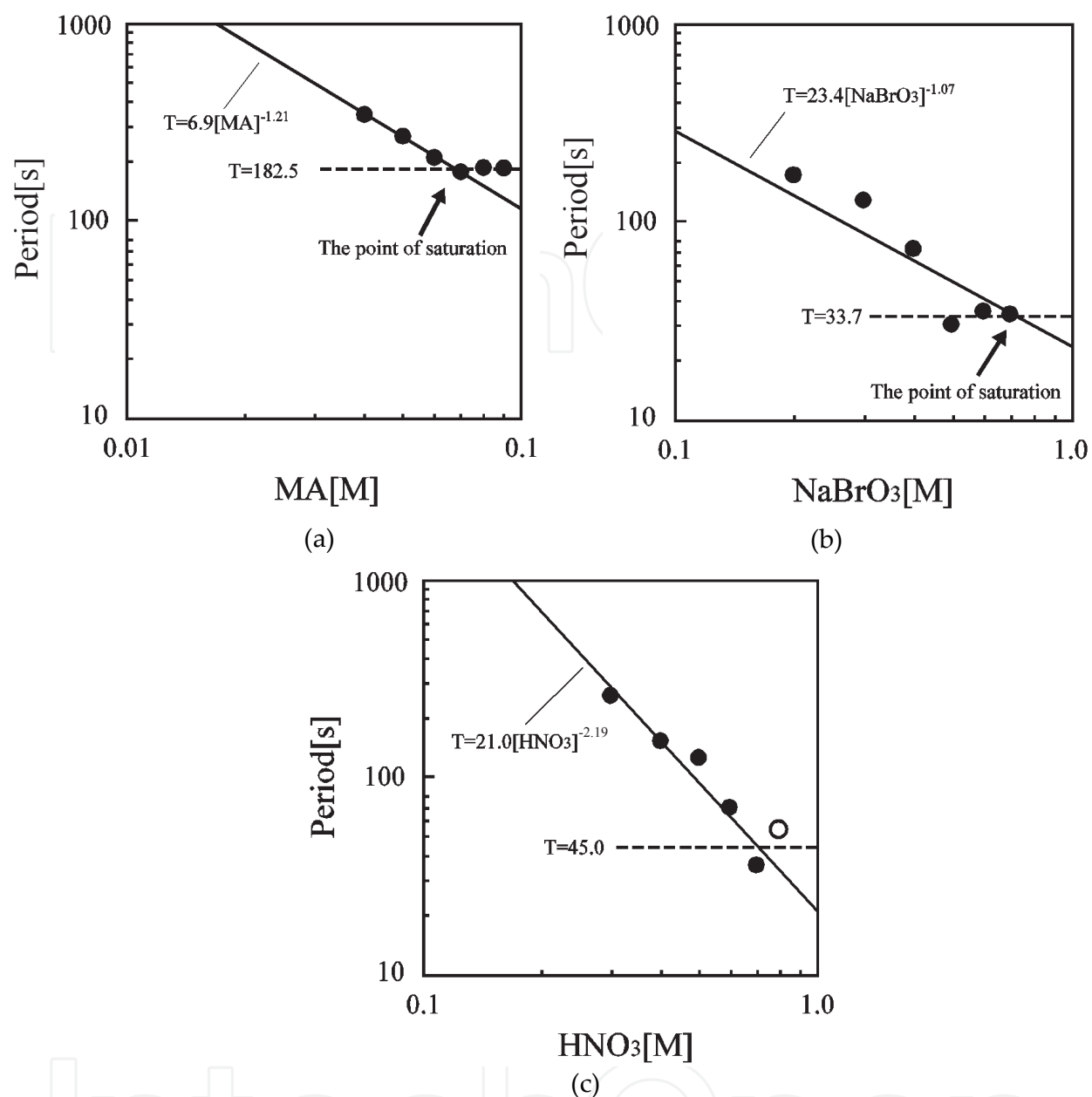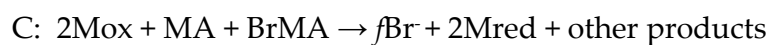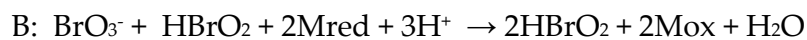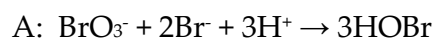
Figure 11. Logarithmic plots of period (T in s) vs initial molar concentration of one BZ substrate at a constant temperature (T=20 °C) under fixed concentrations of the other two BZ substrates; (a) [NaBrO₃] = 0.084M and [HNO₃] = 0.3M, (b) [MA] = 0.0625M and [HNO₃] = 0.3M, (c) [MA] = 0.0625M and [NaBrO₃] = 0.084M. (●) plots and (○) plots show the linear relation and the saturated line vs initial concentration of one BZ substrate, respectively. (Reprinted ref. 57, Copyright American Chemical Society. Reproduced with permission.)

main processes: consumption of Br⁻ ions (process A), autocatalytic formation of HBrO₂ (process B), and formation of Br⁻ ions (process C).

A: $BrO_3^- + 2Br^- + 3H^+ \rightarrow 3HOBr$
B: $BrO_3^- + HBrO_2 + 2Mred + 3H^+ \rightarrow 2HBrO_2 + 2Mox + H_2O$
C: $2Mox + MA + BrMA \rightarrow fBr^- + 2Mred + other\ products$

In the process of B and C, the Ru(bpy)₃ moiety in the gel works as the catalyst: the reduced Ru(bpy)₃ moiety is oxidized (process B), and the oxidized one is reduced (process C). Therefore, as the initial concentration of the MA increased, the mole fraction of the reduced Ru(bpy)₃ moiety in the gel increased in accordance with the FKN mechanism. With increasing in the mole fraction of the reduced Ru(bpy)₃ in the gel, the shrinking force originating in the hydrophobic reduced Ru(bpy)₃ greatly increased as well. Generally, as for a polymer gel, deswelling speed is faster than the swelling one. Once the gel collapsed, it takes a lot of time for the aggregated polymer domain in the gel to recover the elongated state. This is because the polymer aggregation state is thermodynamically more stable in the polymer gel. Therefore, as the shrinking force increased, the swelling speed of the poly(VP-*co*-Ru(bpy)₃) gel significantly decreased. As a result, in the higher MA condition, the period at the saturated point was long (T=182.5) compared with the other condition (T=33.7 (Figure 11(b)) and T=45.0 (Figure 11(c)). On the other hand, in the case of Figure 11(b), the period at the saturated point was greatly shorter than that in Figure 11(a). In the condition of Figure 11(b), the swelling force originating in the hydrophilic oxidized Ru(bpy)₃ moiety increased due to the increase in the mole fraction of the oxidized Ru(bpy)₃ moiety in the gel in accordance with the FKN mechanism. Therefore, the gel can cause the swelling-deswelling self-oscillation at the high speed due to the strong recovering force originating in the higher mole fraction of the hydrophilic oxidized Ru(bpy)₃ moiety in the gel. Moreover, in the condition of Figures 11(c), the period for the poly(VP-*co*-Ru(bpy)₃) gel had the different aspect from that of the conventional-type poly(NIPAAm-*co*-Ru(bpy)₃) gel.[75] The period of the self-oscillation decreased with increasing the initial concentration of the BZ substrates because of the increase in the collision frequency among the BZ substrates. Therefore, we considered that the relationship between the period and the [HNO₃] for the poly(VP-*co*-Ru(bpy)₃) gel is of a more natural tendency. In addition, in the condition of Figure 11(c), the control range of the period by changing the initial concentration of the HNO₃ for the gel was much wider than that for the poly(NIPAAm-*co*-Ru(bpy)₃) gel. [75]

Moreover, as shown in Figure 12, the period of the swelling-deswelling self-oscillation decreased with increasing the temperature because the temperature affects the BZ reaction rate in accordance with the Arrhenius equation.[30] The period of the swelling-deswelling self-oscillation to the temperature for the poly(VP-*co*-Ru(bpy)₃) gel has the linear relationship. The period (2 second) reached the saturation at 46 °C in the BZ condition ([MA] = 0.08M, [NaBrO₃] = 0.48M and [HNO₃] = 0.48M). This is because the swelling-deswelling speed of the gel is slower than the changing rate of the redox states of the Ru(bpy)₃ in the gel. That is, the self-oscillating behavior of the gel cannot follow the changing the redox state of the Ru(bpy)₃ moiety. The maximum frequency (0.5Hz) of the poly(VP-*co*-Ru(bpy)₃) gel was 20 times as large as that of poly(NIPAAm-*co*-Ru(bpy)₃) gel. [75] The self-oscillating behaviors of the poly(VP-*co*-Ru(bpy)₃) gel at 20°C and 50°C were shown in the Figure 12(b) and 12(c), respectively. The displace of the volume change self-oscillation at 20°C and 50°C were about 10 μm and 4 μm, respectively. These results clarified that the displacement of the swelling-deswelling self-oscillation for the gel has the trade-off relationship against the period of the self-oscillation, that is, the length of the volume change decreased with increase in the period.
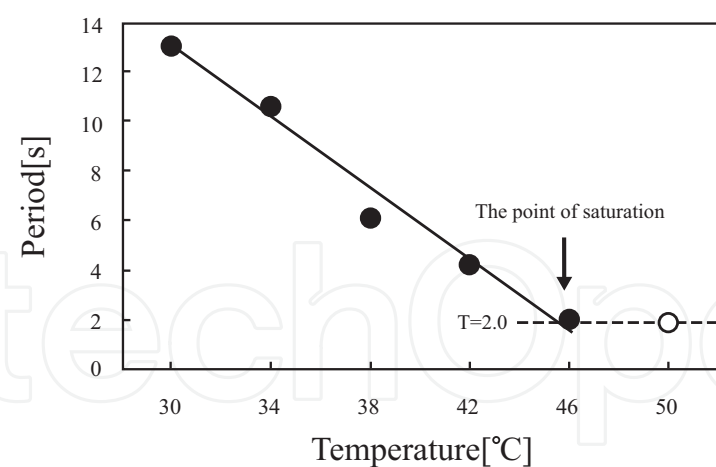
(a)
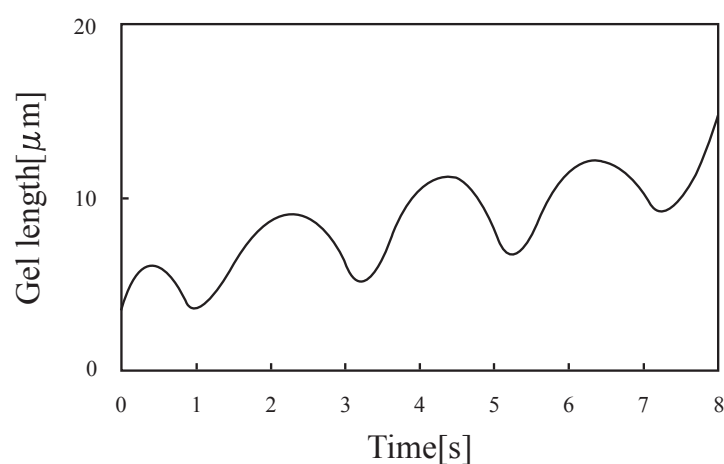
(b)
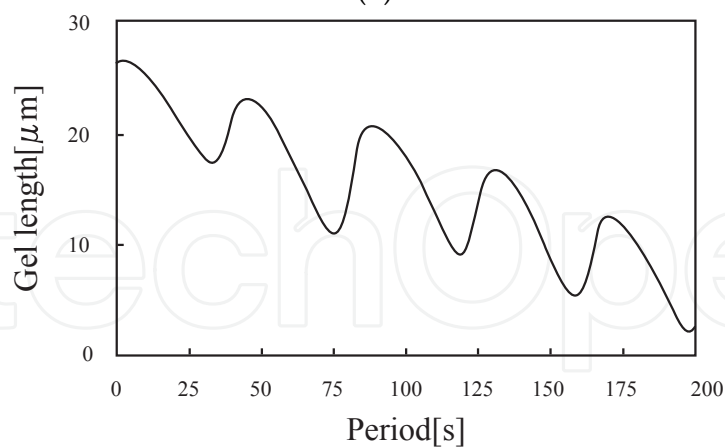
(c)

Figure 12. (a) Dependence of the self-oscillation period on the temperature. (●) plots and (○) plots show the linear relation and the saturated line vs temperature, respectively. (b) Self-oscillating profile of cubic poly(VP-*co*-Ru(bpy)₃) gel at 50°C (MA = 0.08M, NaBrO₃ = 0.48M and HNO₃ = 0.48M). (c) Self-oscillating profile of cubic poly(VP-*co*-Ru(bpy)₃) gel at 20°C (MA = 0.08M, NaBrO₃ = 0.48M and HNO₃ = 0.48M). Cubic gel (each side length is about 2mm and 20mm) was immersed in 8ml of the mixture solution of the BZ substrates. (Reprinted ref. 57, Copyright American Chemical Society. Reproduced with permission.)

3.3. Tubular gel motility driven by chemical reaction networks

In previous studies, De Kepper *et al.* showed a method to form the contraction waves by coupling the pH-responsive hydrogel and the acid autocatalytic chlorite tetrathionate (CT) reaction [42, 43]. They presented a system specially designed to show the chemomechanical instabilities, in other words, dynamical deformations of the functional gels, such as contraction waves and complex spatio-temporal volume oscillations. However, in this system, the pH responsive cylindrical gel is fixed to continuous stirred tank reactors (CSTR) because it must be permanently fed with constant flows of fresh CT reactants. Therefore, this system is unsuitable for the development of a locomotive gel robot. It is necessary to develop a novel concentration tuning mechanism without the stirred reactor for the coupled system of the functional gel and the CT reaction.
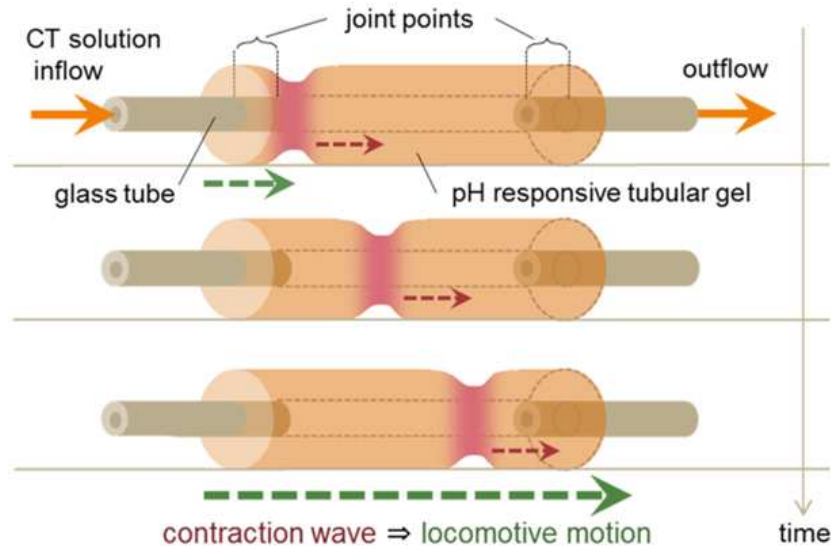

Figure 13. Schematic representation of the principles of the tubular gel feeding system (Reprinted ref. 58, Copyright *IEEE*. Reproduced with permission.)

In this chapter, we introduce a novel pH-responsive tubular gel and propose a new method of generating contraction waves on the functional gel. Figure 13 shows the schematic representation of the principle of the feeding system of the tubular gel. We controlled the reaction diffusion system by pouring the reactant solution into the hollow of the tubular gel, and attempted to achieve the peristaltic movement of the tubular gel by formulating contraction wave. This system enables us to feed with constant flow of fresh reactants, and also to be free from tank reactors.

The CT reaction is known as the acid autocatalytic reaction with the concentration changes of various sorts of reactive substrates, including the chlorite and tetrathionate ion, and this reaction exhibits a bi-stability of an acid steady state and an alkaline steady state. The CT reaction shows very complex kinetics which is still not completely understood [76]. However, it can be described by the following chemical reaction,

$$7ClO_2^- + 2S_4O_6^{2-} + 6H_2O \rightarrow 7Cl^- + 8SO_4^{2-} + 12H^+.$$
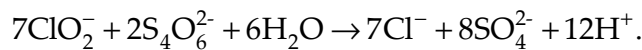
It runs in slight chlorite excess, and is associated with the following autocatalytic empirical rate law,

$$r = -\frac{1}{7}\frac{d[ClO_2^-]}{dt} = k[ClO_2^-][S_4O_6^-][H^+]^2,$$

r indicates the concentration per unit mol of the reactive substrates, and k is a proportionally coefficient. The changes between the steady states of the CT reaction take place depending on the feeding condition of the proton. When an alkali is constantly supplied, the CT reaction solution can maintain an alkaline steady state. As an acid perturbation is added or an alkali supply decreases below a certain concentration, the acid autocatalytic reaction develops and acid region spreads by the reaction-diffusion process, finally the solution becomes acid steady state. When autocatalytic reactions are operated in a pH responsive spherical gel, the gel shrinks following the one-way reaction, regularly. However, in some conditions, the relatively faster diffusivity of the proton can lead to the oscillatory reaction diffusion instability [42,43,77,78]. The volume oscillation of spherical gel is generated by coupling the CT reaction with the volume phase transition of the pH-responsive gel, and we call the concatenation of the two phenomena "chemical reaction networks."
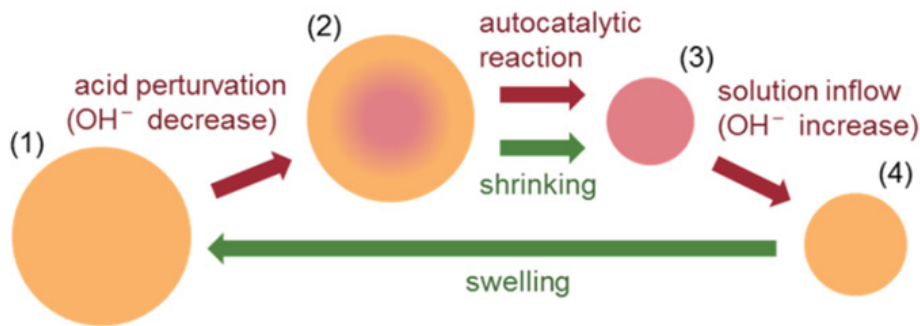

Figure 14. Flowchart of the chemical reaction networks. Each disk shows the condition of a spherical gel. The red arrows indicate changes of the interior CT solution and the green arrows indicate volume phase transition of the pH-responsive gel, that is, the gel causes shrinking or swelling. (Reprinted ref. 58, Copyright *IEEE*. Reproduced with permission.)

Figure 14 shows the flowchart of the chemical reaction networks. The red areas indicate the acid steady state and the yellow areas indicate the alkaline steady state. There are four steps in the networks:

1. The spherical gel is in the uniform alkaline steady state.
2. When the gel radius grows and exceeds a certain threshold value, an acid perturbation rises in the core of the gel.
3. The acid region fills the gel entirely, and the gel shrinks.
4. When the gel radius shrinks below a certain threshold value, it swells again by inflowing of alkali solution.

As described above, the stabilities of such steady states depend on the gel radius. It is shown theoretically and experimentally that the switching between the chemical reaction networks

occurs with hysteresis as a function of such geometric parameters. In this case, the reaction diffuses symmetrically from the center of the gel. When the reaction is applied to the cylindrical gels or tubular gels, it diffuses symmetrically to the diameter direction and also diffuses to the length direction. The disks shown in Figure 14 indicate the changes of the cross-section surface at one location of the cylindrical gel.

For coupling pH-responsive gels and the CT reaction, it is quite important to achieve large volume changes of the gels, because the stabilities of the steady states depend on the gel sizes. Also, the speed of volume change has a high correlation with the contraction wave shape. However, in general, the reactivities of hydrogels composed of chemically cross-linked polymer networks are low because the polymer chains are molecularly restricted by a large number of cross-links. An *N*-isopropylacrylamide (NIPAAm) gel with a microscale phase separation that underwent a quick response has previously been reported [79]. By preparing a NIPAAm gel above the LCST, the NIPAAm gel forms a porous structure with polymer-rich domains and aggregations in the matrix of loosely bound network structures [80]. Consequently, polymer-rich domains inside the gel aggregate or disperse rapidly through the porous structure within the gel by an effluent pathway of the solvent. Therefore, in this investigation, we prepared the microphase-separated AAm-based gels. The microphase-separation in the gel depends strongly on the methods of gel preparation. Meanwhile, a method for preparing the microphase-separated gels by altering the composition of the solvent has been reported [55]. Therefore, we synthesized the poly (AAm-*co*-AAc) gels in water/acetone solvents. Also, we investigated the gels kinetics at the different mixture proportions of the solvents.
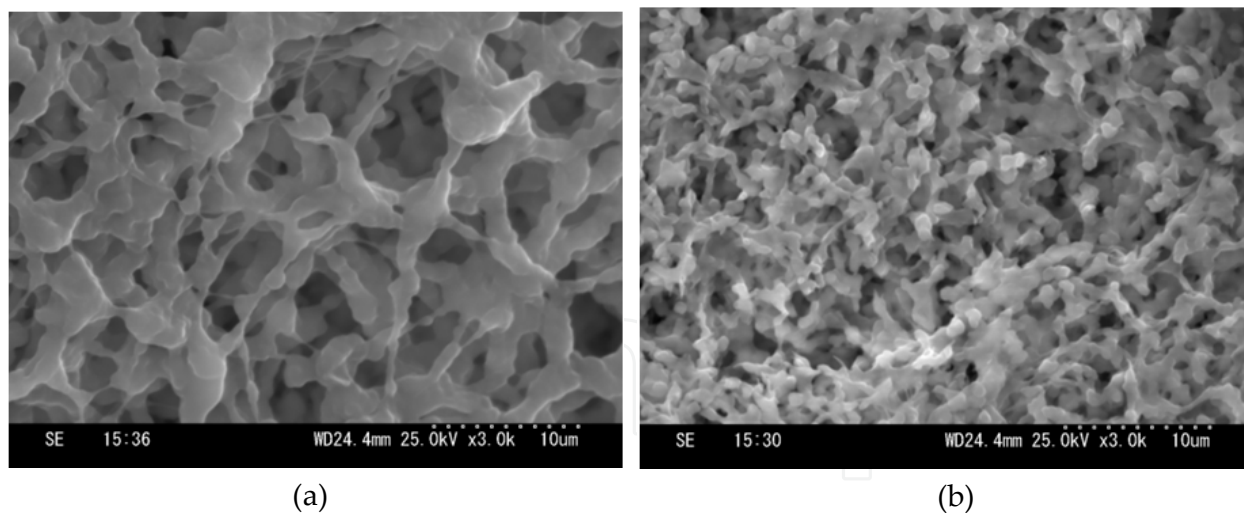

(a)   (b)

Figure 15. SEM images of the interior morphologies of poly (AAm-*co*-AAc) microphase-separated gel with the mixing ratio of water/acetone solvents at 50/50 ((a) swelling state and (b) shrinking state at equal magnification). (Reprinted ref. 58, Copyright *IEEE*. Reproduced with permission.)

First, we observed the structures of the gels. Figure 15 shows the SEM images of the interior morphologies of the poly(AAm-*co*-AAc) microphase-separated gels with the mixing ratio of water/acetone solvents at 50/50. There are polymer rich domains inside the both gels (swelling state and shrinking state) and their sizes change in proportion as the volume

phase transitions of the gels. This microscale structures are quite different from those of ordinary poly(AAm-*co*-AAc) gels with water solvents.

Next, we investigated the phase transition kinetics of the poly(AAm-*co*-AAc) cylindrical gels. When the external pH was rapidly changed, the gel diameters gradually changed to approach the equilibrium state. Figure 16 shows the plots of the gel diameters as a function of time on the shrinking process. Here, let us define L_f, $L(t)$ and L_i, as the final gel diameter, the gel diameter at t = t and the initial gel diameter (t = 0), respectively. The time evolution was found to be well described by a single exponential:

$$L(t) = L_i - \Delta L(1 - e^{-(t/\tau)}) \tag{1}$$

where ΔL and τ represents the total gel length change ($=L_i - L_f$) and the characteristic time of shrinking. When τ and L_f are determined, we can estimate the diffusion constant D by using the following relation for cylindrical gels [81]:

$$D = \frac{L_f^2}{24\tau} \tag{2}$$

From the results, the corrective diffusion constant of the poly(AAm-*co*-AAc) cylindrical gels can be estimated as follows; (A) 4.39×10^{-5} mm²/s, (B) 5.38×10^{-5} mm²/s, (C) 1.75×10^{-3} mm²/s, (D) 1.99×10^{-3} mm²/s, (E) 2.07×10^{-3} mm²/s. In the case of sample (A) and (B), the corrective diffusion constants are almost the same as those of the normal type hydrogels. On the other hand, in the case of sample (C), (D) and (E), they are two orders of magnitudes larger than those of sample (A) and (B). These results indicate that the mixture fractions of acetone to the solvents have the threshold values for the microphase-separation. Also, these results confirm that the microphase-separation plays an important role for increasing speed of the volume phase transition.

We also investigated the detailed pH-responsiveness of the gels. Figure 17 shows the equilibrium swelling of the poly (AAm-*co*-AAc) cylindrical gels at various pH values. From this results, all samples caused volume phase transition between the pH variation range of the CT reaction (from pH = 2 to pH = 11). Also, the diameter change rates of sample (A) and (C) are larger than that of sample (E). It is notable that the stiffness of the gels depends on the mixture proportions of water/acetone solvents. The stiffness of the gels tends to get lower as the mixture fractions of acetone increase. In this experiment, sample (D) and (E) do not stand up under their own weight and became easily deformed in air. Therefore, for this reason, we chose sample (C) as the material of the tubular gel because of its stiffness and phase transition kinetics.

We succeeded in coupling the pH-responsive hydrogel and the CT reaction. Figure 18 shows the propagation of the acid region in the swollen part of the tubular gel. The mixture proportion of the solvent of the tubular gel was same as sample (C). As shown in Figure 18, the CT solution was colored with methyl red. The yellow area corresponds to alkaline composition and the red area corresponds to acid composition. The red allows indicate the

forefront of the acid region and the green allows indicate the forefront of the gel contraction. When the acid perturbation was applied to the left part of the tubular gel, the red area propagated to the right, and finally covered the entire gel. Also, the gel diameter shrank following the propagation of the acid region, as shown in Figure 18. These results suggest that the poly(AAm-*co*-AAc) tubular gel can be coupled with the CT solution, in terms of the acid propagation and the volume change of the gel.
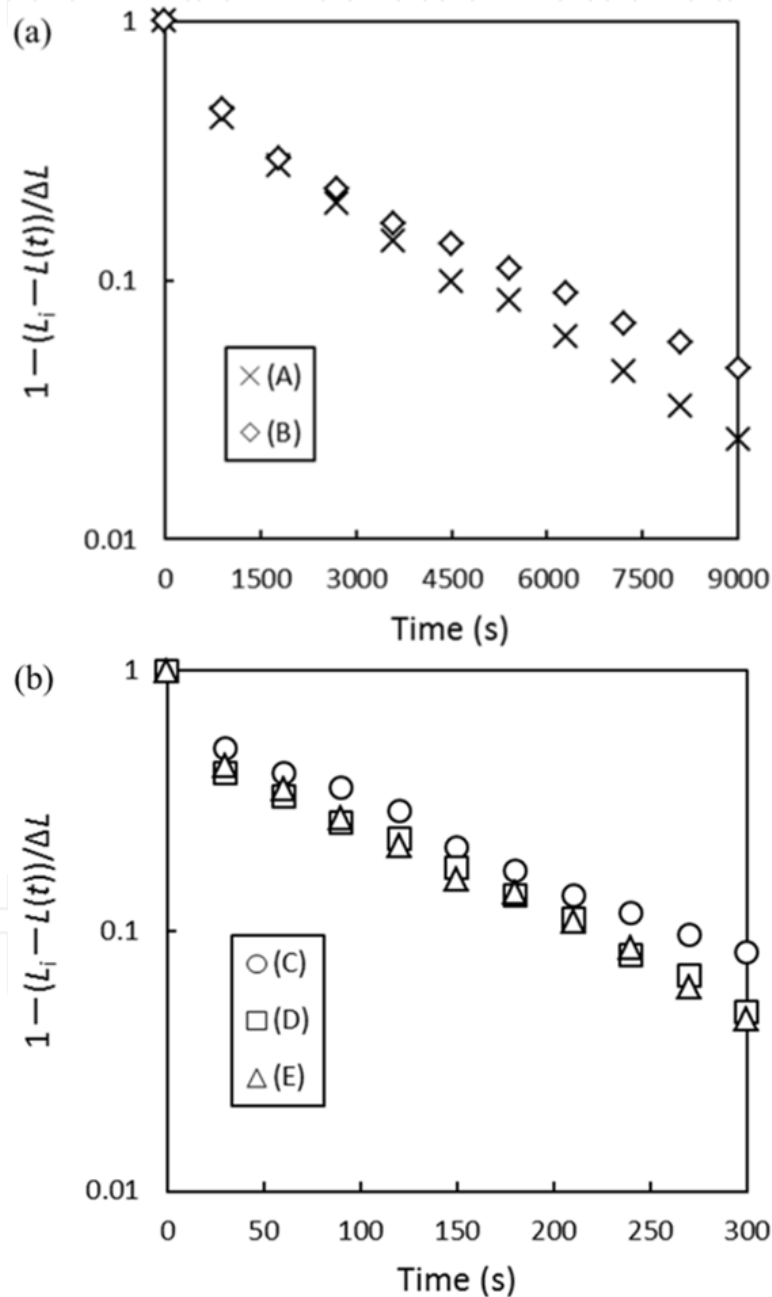

Figure 16. Shrinking behaviors of poly(AAm-*co*-AAc) cylindrical gels at the different mixture proportions of water/acetone solvents ((a): (A) 100/0, (B) 80/20, (b): (C) 70/30, (D) 60/40, and (E) 50/50 wt %). (Reprinted ref. 58, Copyright *IEEE*. Reproduced with permission.)
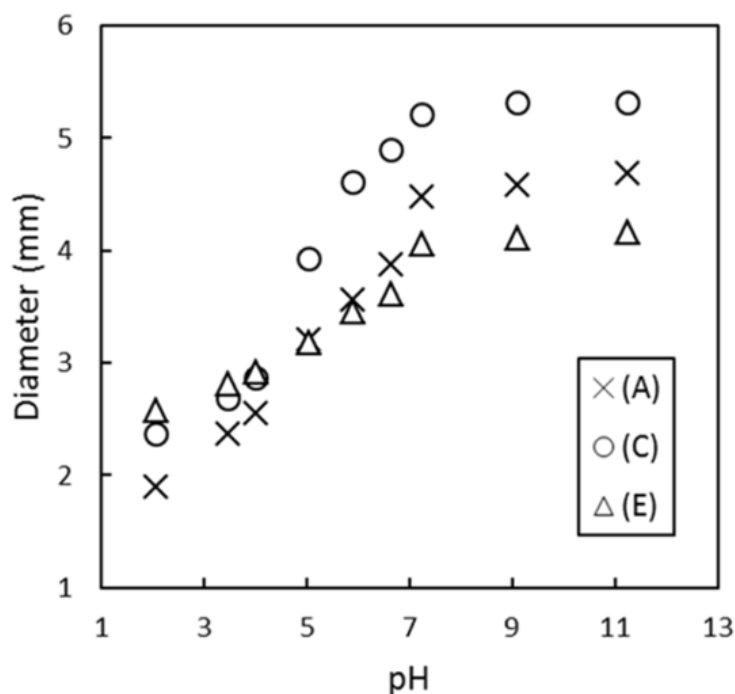
Figure 17. Equilibrium swelling of poly(AAm-*co*-AAc) cylindrical gels at various pH values adjusted using HCl and NaOH solutions, at the different mixture proportions of water/acetone solvents ((A) 100/0, (C) 70/30, and (E) 50/50 wt %). (Reprinted ref. 58, Copyright *IEEE*. Reproduced with permission.)

Fig. 19 shows the spatiotemporal diagram constructed from sequential images of the acid propagation. The extractive line is the black bar in Figure 18 (a). As shown in Figure 19, the acid region propagates at the constant speed, and the velocity of the acid propagation was 16 μm/s. It is 10 times faster than that of the previous research [42]. We also measured the velocity of the acid propagation in the mixed CT solution in the glass tube, and it was 200 μm/s. This is much larger value than that in the case of Figure 18. This result indicates that the propagation occurred inside the gel. These results confirm that a part of the chemical reaction networks, from step (1) to step (3) in Figure 14, was realized experimentally. In order to achieve autonomous swelling of the gel, from step (3) to step (4) in Figure 14, the gel diameter needs to shrink below a certain threshold value. It means that the minimum and maximum sizes of the tubular gels should be regulated for realizing oscillatory volume changes by inflowing of alkali in the CT solutions. The concentrations or mixing ratios of the CT solutions also affect the forming of the chemical reaction networks. The regulation of the gel sizes and the CT solutions will take an important role in the generation of the contraction waves in the tubular gels. This research will be the first step for realizing the biomimetic chemical robot which causes peristaltic locomotion.
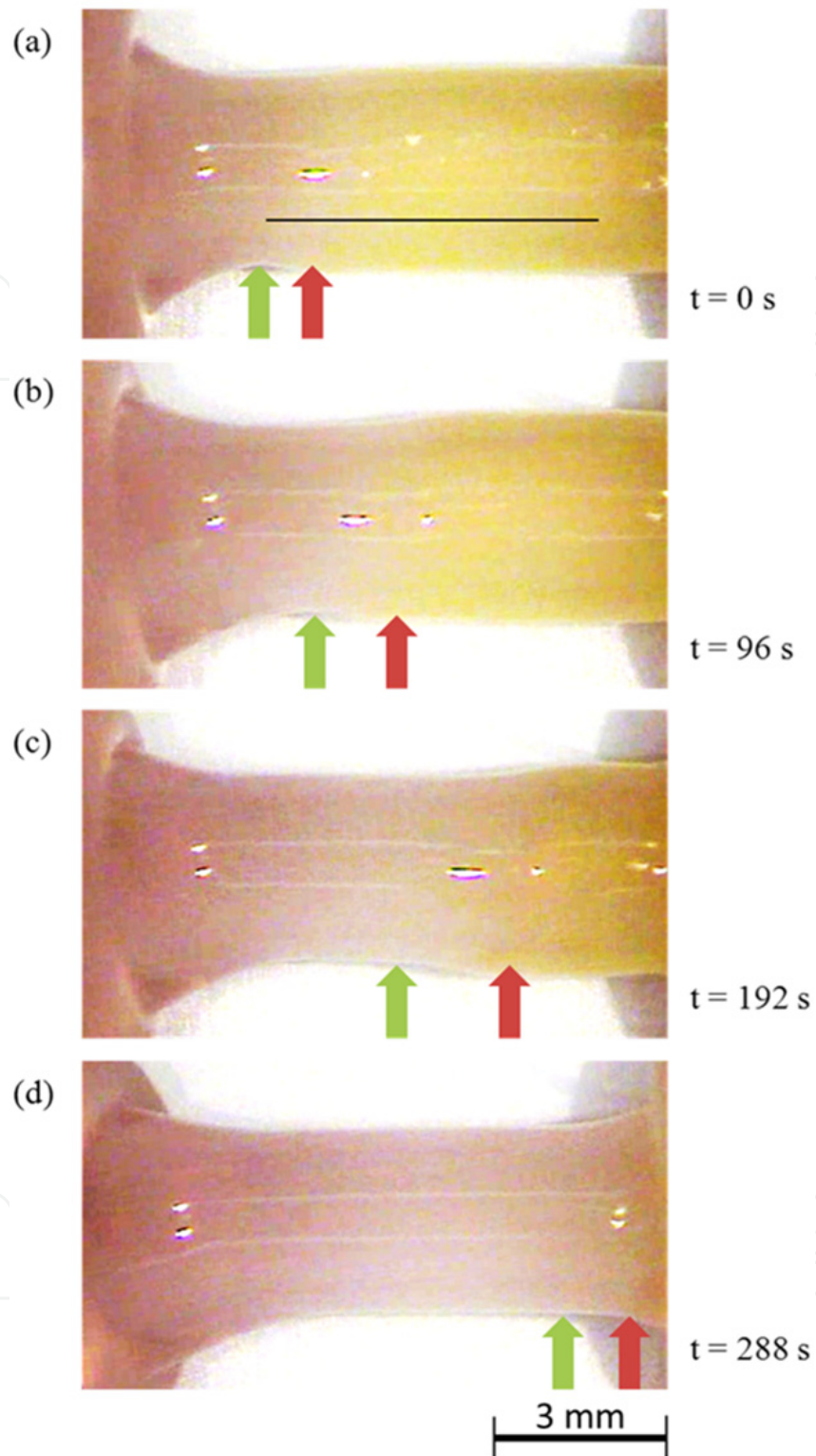
Figure 18. Propagation of the acid front in the swollen part of the tubular gel. An acid perturbation was applied to the left part of the gel. The yellow area corresponds to alkaline composition and the red area corresponds to acid composition. The red allows indicate the forefronts of the acid regions and the green allows indicate the forefronts of the gel contraction, which are the rightmost points obtained locally minimum diameters. (a) t = 0 indicates the criterion time after applying the acid perturbation. (Reprinted ref. 58, Copyright *IEEE*. Reproduced with permission.)
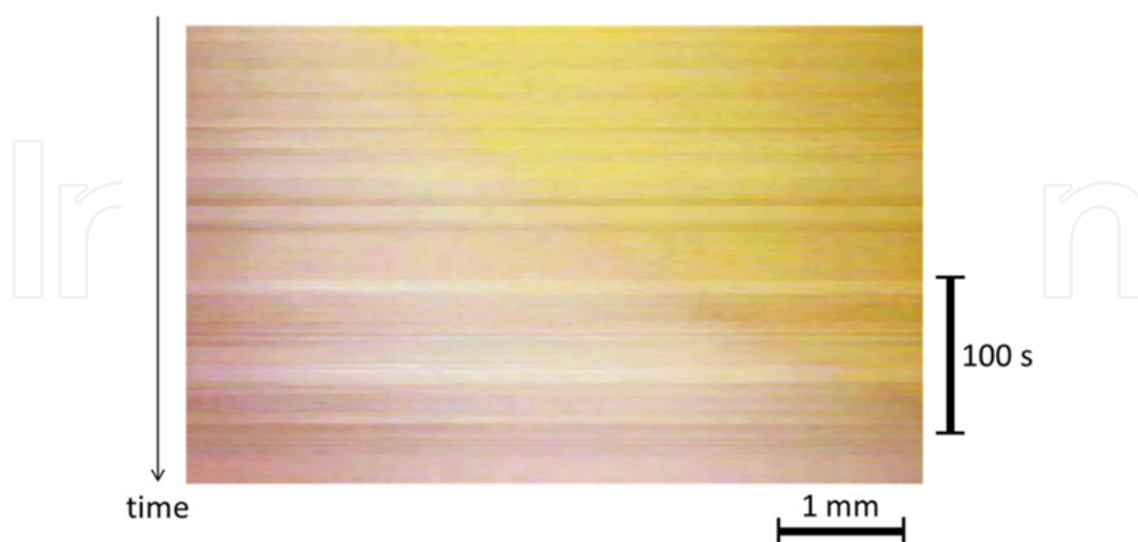
Figure 19. Spatiotemporal diagram constructed from sequential images of the acid propagation. The extracted horizontal lines correspond to the black bar in Fig. 18 (a). (Reprinted ref. 58, Copyright *IEEE*. Reproduced with permission.)

3.4. A pendulum-like motion of nanofiber gel actuator synchronized with external periodic pH oscillation

In this study, in order to drive the nanofiber gel actuator in response to the external pH changes, we selected the pH responsive poly(AAc) (PAAc) as a main polymer chain. The PAAc is protonated when the pH is below the pKa. When the pH of the solution is below pKa, the nanofiber gel collapses due to hydrogen bonding among the polymer chains. On the other hand, when the pH is above the pKa, the PAAc polymer chain is ionized, that is, the solubility of the polymer chain changes from a hydrophobic to a hydrophilic nature. As a result, the nanofiber gel expands because of the electrostatic repulsion force among the charged PAAc polymer chains. However, the fiber gel that consists of the only PAAc polymer chain, finally dissolves into the aqueous solution because the gel does not have the cross-linkage among the polymer chains into the nanofiber. In order to avoid the nanofiber gel dissolving, especially when it is above the pKa, we adopted the tBMA domain into the PAAc as a cross-linkage and a solubility control site, due to the hydrophobic interaction among the tBMA in the nanofiber. As a result, the poly(AAc-*co*-nBMA) nanofiber gel does not dissolve in the aqueous solution.

Figure 20 shows distributions of diameter of the poly(AAc-*co*-nBMA) nanofibers electrospun at two flow rates (2.0 mL/h and 1.0 mL/h) (See Figure 21). In general, the fiber diameters depend on the flow rate. In our experiment, the average diameter at the flow rate 2.0 mL/h (302 nm) was thicker than at 1.0 mL/h (233 nm).
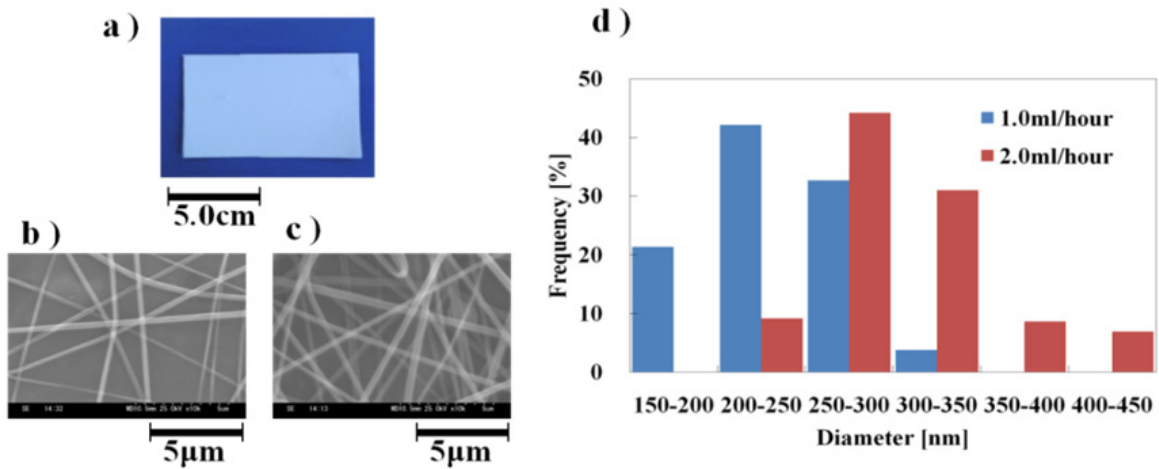
Figure 20. (**a**) An electrospun fiber sheet. (**b**) The SEM image of nanofibers at flow rate 1.0 mL/h. (**c**) The SEM image of nanofibers at flow rate 2.0 mL/h. (**d**) Distribution of fiber diameters of poly(AAc-*co*-nBMA) nanofibers electrospun at different flow rates.
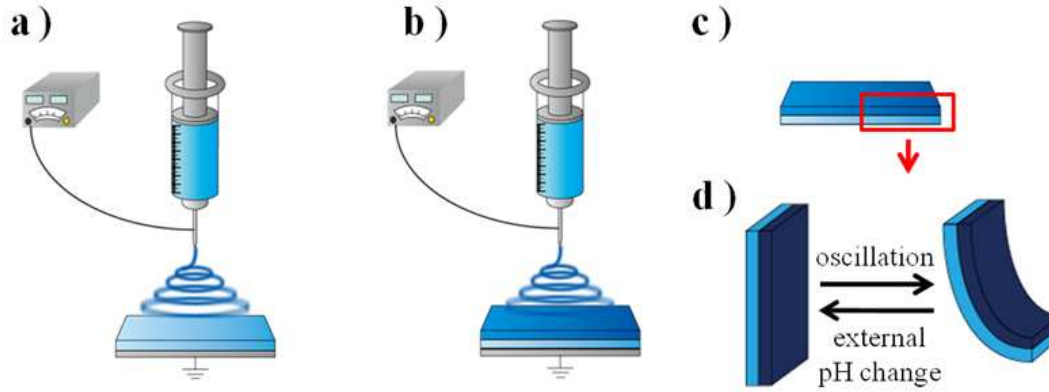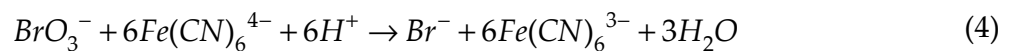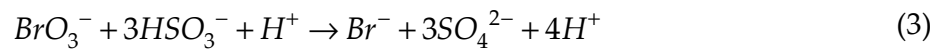

Figure 21. The method of introducing the anisotropic structure into the nanofiber gel.
(**a**) Electrospinning at a flow rate of 2.0 mL/hour (sprayed for 30 minutes). (**b**) Electrospinning at a flow rate of 1.0 mL/hour (sprayed for 60 minutes). (**c**) Drying in 50 °C over night. (**d**) Cutting into 15 mm × 3 mm × 200 μm.

In order to drive the nanofibrous gel actuator synchronized with autonomous pH oscillation, we focused on the Landolt pH-oscillator, based on a bromated/ sulfite/ ferrocyanide reaction discovered by Edblom *et al.* [39,40]. This reaction causes the autonomous cyclic pH changes with a wide range at room temperature. The reaction has many reaction steps, so we estimated the main reactions as follow [41].

$$BrO_3^- + 3HSO_3^- + H^+ \rightarrow Br^- + 3SO_4^{2-} + 4H^+ \tag{3}$$

$$BrO_3^- + 6Fe(CN)_6^{4-} + 6H^+ \rightarrow Br^- + 6Fe(CN)_6^{3-} + 3H_2O \tag{4}$$

In Process (1), H_2SO_3 is oxidized by bromate, and ferrocyanide is oxidized by bromate in Process (2). In the above two processes, the hydrogen ions produced and consumed at comparable rates. Therefore, in this reaction, the pH oscillation takes place in the CSTR. Figure 22 shows the experimental set up of the CSTR. The CSTR was constructed by using

four peristaltic pumps in order to feed four solutions of potassium bromated, sodium sulfite, potassium ferrocyanide and sulfuric acid. Moreover, this system had one more peristaltic pump to drain the excess solution. The degree of changing the pH range (amplitude) and period of the oscillating reaction can be controlled by changing the feed concentration, flow rate and solution temperature.
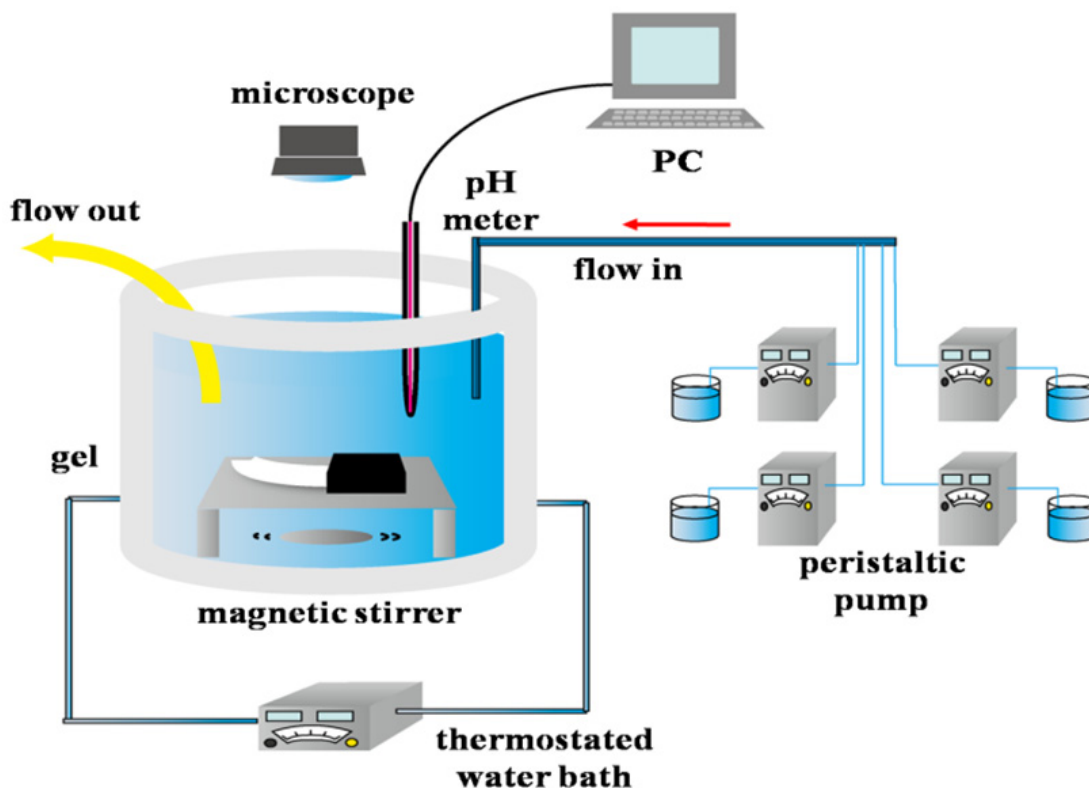

Figure 22. Continuous monitoring system for oscillation: monitoring both the medium pH and the gel motion in a CSTR.

Figure 23 shows a motion of the nanofiber gel actuator. The bending and stretching motions of the gel actuator synchronized with the pH oscillating reaction. As shown in Figure 23, we defined R as the length between two edges of the gel. Figure 24 shows the trajectory of the nanofiber gel strip. As shown in Figure 24, the gel strip caused the pendulum-like motion. As the external pH is below the pKa, the nanofiber gel stretches because of the deswelling originating from the hydrogen bonding ($1\rightarrow3$). Next, when the pH is above the pKa, the gel bends because of the swelling originating from the repulsive force among the anionic polymer chains ($4\rightarrow6$).

Figure 25 shows the temporal changes of R of the gel strip and the external pH, respectively. The range of the pH oscillation based on a bromate/sulfite/ferrocyanide reaction was $3.1 < pH < 7.2$, and the period was about 20 min. When the external pH changes periodically, the R of the gel strip cyclic changes synchronized with the external pH change. As shown in Figure 25, when the pH sharply decreased, the R of the gel strip starts to increase because the gel collapsed. Next, when the pH increased rapidly, R gradually decreased, due to the

gel actuator swelling originating from the repulsive force of AAc domain in the polymer chain. That is because the gel has different rates at swelling and deswelling. In general, the swelling motion of the gel is slower than the deswelling motion. Therefore, when the gel actuator bended, the R value gradually decreased.
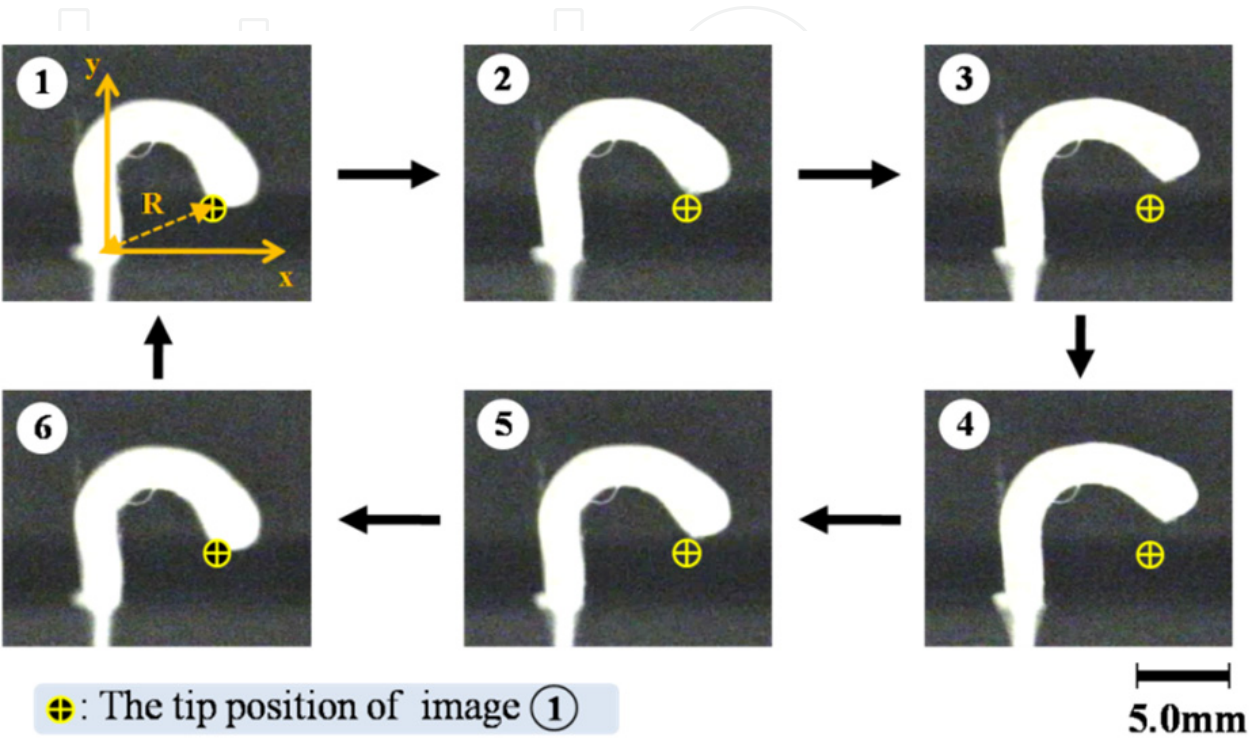

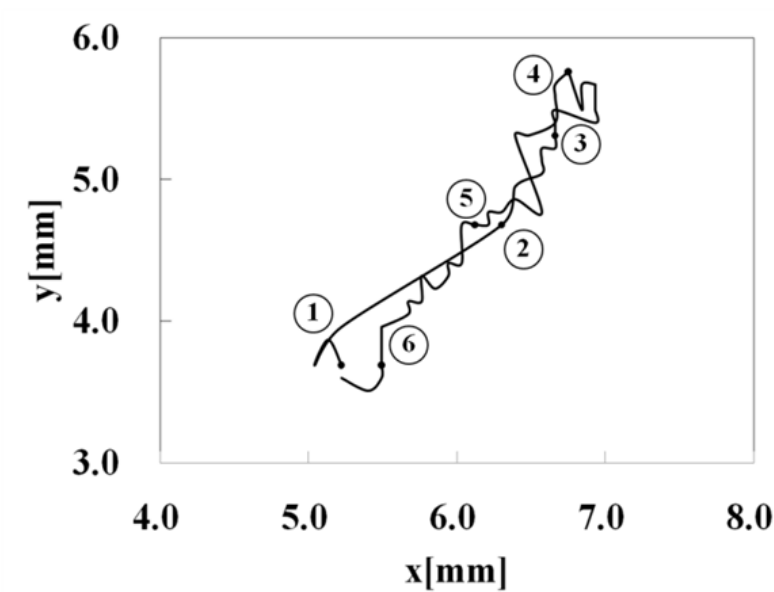**Figure 23.** Periodical pendulum motion of poly(AAc-*co*-nBMA) nanofiber gel.

Figure 24. Trajectory of the tip of the gel relative to its attachment position during pH oscillation.
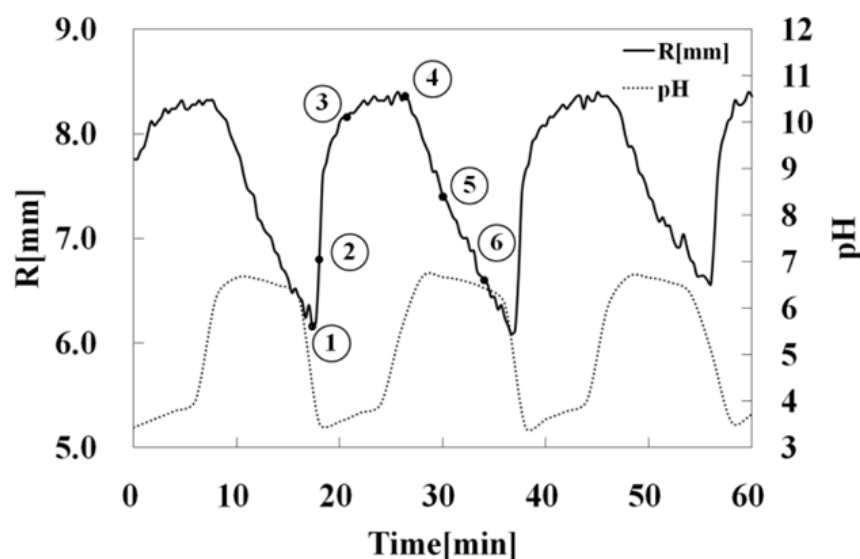
Figure 25. The time series of pH (discontinuous line) and R (solid line).

4. Conclusion

As for the VP-based self-oscillating polymer chain, we examined the influence of initial substrate concentrations of the BZ reaction on transmittance self-oscillation for the novel poly(VP-*co*-Ru(bpy)₃) solution. As a result we noted that the width of the self-oscillation is much affected by the initial concentration of the BZ substrates. In addition, we clarified that the amplitudes of the transmittance self-oscillation is hardly affected by the initial concentrations of the BZ substrates. This tendency was not observed in the case of the AMPS-containing polymer solution. Furthermore, we demonstrated that the period of the transmittance self-oscillation can be controlled by the selection of the initial concentration of the BZ substrates.

Furethermore we succeeded in clarifying the influence of the initial concentration of the BZ substrates and the temperature on the period of the swelling-deswelling self-oscillation for the novel poly(VP-*co*-Ru(bpy)₃) gel. The logarithmic plots of the period against the initial concentration of one BZ substrate under fixed the other two BZ substrates showed the good linear relationships. Moreover, the period of the self-oscillation increased with the increasing the temperature in accordance with Arrenius equation. The maximum frequency (0.5Hz) of the poly(VP-*co*-Ru(bpy)₃) gel was 20 times as large as that of poly(NIPAAm-*co*-Ru(bpy)₃ gel. Therefore, the period of the swelling-deswelling self-oscillation for the gel can be controllable in wide range by optimizing the initial concentration of the three BZ substrates and the temperature. In addition, we showed that the displacement of the self-oscillation for the gel has the trade-off relationship against the period of the self-oscillation.

Next, we introduced the new method of generating contraction waves in the functional gel, which controls the reaction diffusion system by flowing the CT solution into the hollow tubular gel. In order to realize this system, the poly(AAm-*co*-AAc) microphase-separated

gels were synthesized with various mixture proportions of the water/acetone solvents. From the view of the swelling kinetics, we experimentally clarified that the suitable mixture proportion for the fast volume changes and the adequate robustness for solution sending. Also, we coupled the poly (AAm-*co*-AAc) microphase-separated tubular gel and the CT solution. Moreover, we successfully demonstrated the propagation of the acidic contraction region of the gel. In the next step, we will accomplish the entire chemical reaction networks for realizing a swelling from the acid contraction region, which leads to a contraction wave in the tubular gel. This research will be the first step for realizing the biomimetic chemical robot which causes a peristaltic locomotion.

Finally, we introduced the fabrication of nanofiber gel actuator with anisotropic internal structure by changing the flow rate in electrospinning. The developed gel generates bending and stretching motion according to the external pH. In order to drive the nanofiber gel actuator automatically, we focused on the pH oscillating reaction based on a bromate/sulfite/ferrocyanide reaction. As a result, we succeeded in causing the bending-stretching motion of the nanofiber gel actuator synchronized with the external pH oscillation. By analyzing the motion of the gel, we found that the gel actuator caused the pendulum-like motion. Moreover, we clarified that the displacement and period of the nanofiber gel were stable, which makes it promising as a molecular device for potential applications.

Author details

Yusuke Hara[*]
Nanosystem Research Institute (NRI), National Institute of Advanced Industrial Science and Technology (AIST), Japan

Shingo Maeda
Shibaura Institute of Technology, Japan

Takashi Mikanohara, Hiroki Nakagawa, Satoshi Nakamaru and Shuji Hashimoto
Department of Applied Physics, Graduate School of Science and Engineering, Waseda University, Japan

5. References

[1] Fukushima, T.; Asaka, K.; Kosaka, A.; Aida, T. (2005). Fully plastic actuator through layer-by-layer casting with ionic-liquid-based bucky gel, *Angewandte Chemie International Edition*, 44, pp.2410-2413, ISSN 1433-7851

[2] Oguro, K.; Kawami, Y.; Takenaka, H. (1992). An actuator element of polyelectrotyte gel membrane-electrode composite, *Bulletin of the Government Industrial Research Institute, Osaka*, 43, pp. 21–24.

---

[*] Corresponding Author

[3]   Otake, M.; Kagami, Y.; Inaba, M.; Kim, B. & Inoue, H. (2002). Motion design of a starfishshaped gel robot made of electro-active polymer gel. *Robotics and Autonomous Systems*, Vol.40, No.2-3, (August 2002), pp. 185-191, ISSN 0921-8890

[4]   Steinberg, I, Z.; Oplatka, A.; Kachalsky, A. (1996). Mechanochemnical engines, *Nature*, 210, pp. 568–571, ISSN 0028-0836

[5]   Feinberg, A. W. Feigel, A. Shevkoplyas, S. S. Sheehy, S. Whitesides, G, M. & Parker, K. K (2007). Muscular thin films for building actuators and powering devices, *Science*, Vol.317, No.5843, (September 2007), pp.1366-1370, ISSN 0036-8075

[6]   Harada, A. ; Kataoka, K. (1999). Chain length recognition: core-shell supramolecular assembly from oppositely charged block copolymers. *Science*, 283, pp. 65-67 ISSN 1095-9203

[7]   Kim, J.; Nayak, S.; Lyon, L. A. (2005). Bioresponsive hydrogel microlenses, *Journal of the American Chemical Society*, 127, pp. 9588–9592 ISSN 0002-7863

[8]   Kwon, G.H.; Park, J.Y.; Kim, J.Y.; Frisk, M.L.; Beebe, D.J.; Lee, S.H. Biomimetic Soft Multifunctional Miniature Aquabots. *Small* 2008, 4, 2148-2153.

[9]   Hoffman, A. S. (2002) Hydrogels for biomedical applications, *Advanced Drug Delivery Reviews*, 43, pp. 3-12, ISSN 0169-409X

[10] Tanaka, T. (1981). Gels, Scientific American.,244, pp.110-116, ISSN 0036-8733

[11] Hirokawa, Y.; Tanaka, T. (1984). Volume phase transition in a non ionic gel, *Journal of chemical Physics*, 81, pp.6379-6380, ISSN *0021-9606*

[12] Ilmain, F.; Tanaka, T., Kokufuta, E. (1991). Volume transition in a gel by hydrogen bonding, *Nature,* 349, pp.400-401, ISSN 0028-0836

[13] Tanaka, T. (1978). Collapse of gels and critical endpoint, *Physical Review Letters*, 40, pp.820-823, ISSN 0031-9007

[14] Suzuki, A.; Tanaka, T. (1990). Phase transition in a polymer gels induced by visible-light, *Nature,* 346, pp. 345-347, ISSN 0028-0836

[15] Kuhn, W. ; Hargity, B. ; Katchalsky, A. & Eisenberg, H. (1950). Reversible Dilation and Contraction by Changing the State of Ionization of High-Polymer Acid Networks, *Nature*, Vol.165, No.4196, (April 1950), pp. 514-516, ISSN 0028-0836

[16] Hu, Z.; Zhang, X. & Li, Y. (1995). Synthesis and Application of Modulated polymer gels. *Science*, Vol.269, No.5223, (April 1995), pp. 525-527, ISSN 0036-8075

[17] Yeghiazarian, L. Mahajan, S. Montemagno, C. Cohen, C. & Wiesner, U. (2005). Directed Motion and Cargo Transport Through Propagation of Polymer-Gel Volume Phase Transitions, *Advanced Materials*, Vol.17, No.15, (August 2005), pp. 1869-1873, ISSN 0935-9648

[18] Huber, D. L.; Manginell, R. P.; Samara, M. A.; Kim, B. & Bunker, B. C. (2003). Programmed Adsorption and Released of proteins in a Microfluidic device, *Science*, Vol.301, No.5631, (July 2003), pp. 352-354, ISSN 0036-8075

[19] Beebe, D. J.; Moore, J. S.; Bauer, J. M.;Yu, Q.;Liu, R. H.;Devadoss, C.; Jo, B. H. (2000). Functional hydrogel structures for autonomous flow control inside microfluidic channels, *Nature,* 404, pp. 588-590, ISSN 0028-0836

[20] Asoh, T.; Matsusaki, M.; Kaneko, T.; Akashi, M. (2008). Fabrication of Temperature-Responsive Bending Hydrogels with a Nanostructured Gradient, *Advanced Materials*, Vol.20, No.11, pp. 2080-2083, ISSN 0935-9648.

[21] Ross, J.; Muller, S. C.; Vidal, C. (1988). Chemical Waves, Science, Vol. 240, pp.460-465, ISSN 1095-9203.

[22] Epstein, I. R.; Showalter, K.(1996). Nonlinear Chemical Dynamics: Oscillations, Patterns, and Chaos, *The Journal of Chemcal Chemistry*, Vol. 100, No. 31, pp.13132-13147, ISSN 1932-7447.

[23] Epstein, I. R. (1995). The Consequences of Imperfect Mixing in Autocatalytic Chemical and Biological Systems, Nature Vol. 374, pp. 321-327, ISSN 0028-0836

[24] Lee, K. J.; Cox, E. C.; Goldstein, R. E. (1996). Competing Patterns of Signaling Activity in Dictyostelium Discoideum. *Physical Review Letters*, Vol. 76, pp. 1174-1177, ISSN 0031-9007.

[25] Shibayama, M.; Tanaka, T. (1993). Volume Phase Transition and Related Phenomena of Polymer Gels, *Advances in Polymer Science*, Vol. 109, pp. 1-62, ISSN 0065-3195.

[26] Landrot, V.; De Kepper, P.; Boissonade, J.; Szalai, I.; Gauffre, F. (2005). Wave Patterns driven bu chemomechanical instabilities in responsive gels, *The Journal of Physical Chemistry B*, Vol. 109, pp. 21476-21480, ISSN 1520-6106.

[27] Boissonade, J. (2003). Efficient Method for Predicting Crystal Structures at Finite Temperature: Variable Box Shape Simulations, *Physical Review Letters*, Vol. 90, pp. 188302 (4pages), ISSN 0031-9007.

[28] Yashin, V, V. & Balazs, A, C. (2006). Pattern formation and shape changes in self-oscillating polymer gels. *Science*, Vol. 314, No.5800, (September 2006) pp.798-801, ISSN 0036-8075

[29] Yashin, V, V. & Balazs, A, C. (2007). Theoretical and computational modeling of self-oscillating polymer gels, The *Journal of Chemical Physics*, Vol.126, No.12, (March2007) pp.124707-1-124707-17 ISSN 0021-9606

[30] Zaikin, A.N.; Zhabotinsky, A.M. (1970). Concentration Wave propagation in two-dimensional liquid-phase self-oscillating system, *Nature*, 225, pp. 535–537, ISSN 0028-0836

[31] Reusser, E.J.; Field, R.J. (1979). The transition from phase waves to trigger waves in a model of the Zhabotinskii reaction, *Journal of the American Chemical Society*, 101, pp. 1063–1071, ISSN 0002-7863

[32] Nicolis, G.; Prigogine, I. (1997). Self Orgainzation in Nonequilibrium Systems; *Wiley: New York, NY, USA.*

[33] Field, R.J.; Burger, M. (1985). Oscillations and Traveling Waves in Chemical Systems; *John Wiley & Sons: New York, NY, USA.*

[34] Field, R.J.; Noyes, R. M. (1974). Oscillations in chemical systems. IV. Limit cycle behavior in a model of a real chemical reaction, *Journal of Chemical Physics*, 60, pp. 1877–1884, ISSN 0021-9606

[35] Gyorgyi, L.; Turanyi, T.; Field, R J. (1990). Mechanistic details of the oscillatory Belousov-Zhabotinskii reaction, *Journal of Chemical Physics*, 94, pp. 7162–7170, ISSN 0021-9606

[36] Turanyi, T.; Gyorgyi, L.; Field, R. J. (1993), Analysis and simplification of the GTF model of the Belousov-Zhabotinsky reaction, *Journal of Chemical Physics*, 97, pp. 1931–1941, ISSN 0021-9606.

[37] Scott, S. K. (1991), Chemical Chaos, *1st ed.; Oxford University Press: Oxford, UK.*

[38] Mori, H. ; Kuramoto, Y. (1997). Dissipative Structures and Chaos, *Springer-Verlag, Berlin.*

[39] Edblom, E.C.; Orban, M.; Epstein, I.R. (1986). A New Iodate Oscillator: The Landolt Reaction with Ferrocyanide in a CSTR. *Journal of the American Chemical Society*, Vol. 108, pp. 2826-2830, ISSN 0002-7863.

[40] Edblom, E.C.; Luo, Y.; Orban, M.; Kustin, K.; Epstein, I.R. (1989) Kinetics and Mechanism of the Oscillatory Bromate-Sulfite-Ferrocyanide Reaction. *The Journal of Physical Chemistry*, Vol. 93, pp. 2722-2727, ISSN 1089-5639.

[41] Crook, J.; Smith, A.; Jones, A.; Ryan, J. (2002). Chemically Induced Oscillations in a pH-Responsive Hydrogel. *Physical Chemistry Chemical Physics*, Vol. 4, pp. 1367-1369, ISSN 1463-9076.

[42] V. Labrot, P. De Kepper, J. Boissonade, I. Szalai, and F. Gauffre, (2005). Wave Patterns Driven by Chemomechanical Instabilities in Responsive Gels, *Journal of Chemical Physics*, vol. 109, No. 46, pp. 21476-21480, ISSN 0021-9606.

[43] J. Boissonade, P. De Kepper, F. Gauffre, and I. Szalai, (2006) Spatial bistability: A source of complex dynamics. From spatiotemporal reaction-diffusion patterns to chemomechanical structures, *Chaos*, Vol. 16, No. 3, pp. 037109 (8pages), ISSN 1054-1500.

[44] Ishiwatari, T.; Kawaguchi, M.; Mitsuishi, M. (1984). Oscillatry reactions in polymer systems, *Journal of Polymer Science Part A: Polymer Chemistry*, 22, pp. 2699-2704 ISSN 0887-624X

[45] Yoshida, R.; Takahashi, T.; Yamaguchi, T.; Ichijo, H. (1996). Self-oscillating gel, *Journal of the American Chemical Society*, 118, pp. 5134-5135, ISSN 0002-7863

[46] Yoshida, R.; Sakai, T.; Ito, S.; Yamaguchi, T. (2002). Self-oscillation of polymer chains with rhythmical soluble-insoluble changes, *Journal of the American Chemical Society*, 124, pp. 8095-8098, ISSN 0002-7863

[47] Hara, Y.; Yoshida, R. Self-oscillation of polymer chains induced by the Belousov-Zhabotinsky reaction under acid-free conditions. *Journal of Physical Chemistry B* 2005, 109, pp. 9451–9454, ISSN 1089-5647

[48] Hara, Y.; Yoshida, R. (2009). Damping behavior of aggregation-disaggregation self-oscillation for a polymer chain, *Macromolecular Rapid Communications*, 30, pp. 1656–1662, ISSN 1521-3927

[49] Hara, Y.; Yoshida, R. (2005). Control of oscillating behavior for the self-oscillating polymer with pH-control site, *Langmuir*, 21, pp. 9773–9776, ISSN 0743-7463

[50] Hara, Y.; Yoshida, R. (2008). A viscosity self-oscillation of polymer solution induced by the BZ reaction under acid-free condition, *Journal of Chemical Physics*, 128, 224904, ISSN 0021-9606

[51] Hara, Y.; Sakai, T.; Maeda, S.; Hashimoto, S.; Yoshida, R. (2005).b Self-oscillating soluble-insoluble changes of polymer chain including an oxidizing agent induced by the Belousov-Zhabotinsky reaction, *Journal of Physical Chemistry B*, 109, pp. 23316–23319, ISSN 1089-5647

[52] Hara, Y.; Yoshida, R. (2008). Self-oscillating polymer fueled by organic acid. *Journal of Physical Chemistry B*, 112, pp. 8427–8429, ISSN 1089-5647

[53] Maeda, S.; Hara, Y.; Yoshida, R.; Hashimoto, S. (2008). Control of the dynamic motion of a gel actuator driven by the Belousov-Zhabotinsky reaction, *Macromolecular Rapid Communications*, 29, pp. 401–405, ISSN 1521-3927

[54] Maeda, S.; Hara, Y.; Sakai. T.; Yoshida, R.; Hashimoto, S. (2007). Self-walking gel, *Advanced Materials*, 19, pp. 3480–3484, ISSN 1521-4095

[55] Maeda, S.; Hara, Y.; Yoshida, R.; Hashimoto, S. (2008). Peristaltic motion of polymer gels, *Angewandte Chemie International Edition*, 47, pp. 6690-6693, ISSN 1433-7851

[56] Hara, Y.; Yoshida, R. (2009). Influence of a positively charged moiety on aggregation-disaggregation self-oscillation induced by the BZ reaction, *Macromolecular Chemistry and Physics*, 210, pp. 2160–2166, ISSN 1022-1352

[57] Nakamaru, S,; Maeda, S. ; Hara, Y.; Hashimoto, S. (2009). Control of Autonomous Swelling-Deswelling Behavior for a Polymer gel. *Journal of Physical Chemistry B*, 2009, 113, pp. 4609-4613, ISSN 1089-5647

[58] T. Mikanohara, S. Maeda, Y. Hara, S. Hashimoto (2011). Tubular Gel Motility Driven by Chemical Reaction Networks", *Proceeding of 2011 IEEE International Conference on Robotics and Biomimetics*, pp.2008-2013, ISBN 978-1-4577-2136-6.

[59] Nakagawa, H. Hara, Y. Maeda, S. & Hashimoto, S. (2010). A Novel Design of Nanofibrous Gel Actuator by Electrospinning, *Proceedings of IEEE Nano* 2010. ISBN 978-4244-7031-0

[60] Nakagawa, H.; Hara, Y.; Maeda, S. & Hashimoto, S (2010). A Pendulum-Like Motion o Nanofiber Gel Actuator Synchronized with External Periodic pH Oscillation, *Polymers*, Vol.3, No.1, (December 2010) pp 405-412, ISSN 2073-4360

[61] R. McNeill Alexander, (2006). Principles of Animal Locomotion, *Princeton University Press*, ISBN: 9780691126340

[62] Stevens, M.M.; George, J.H. Exploring and Engineering the Cell Surface Interface. *Science* 2005, 310, 1135-1138.

[63] Cui, Y.; Wei, Q.; Park, H.; Lieber, C.M. (2001). Nanowire Nanosensors for Highly Sensitive and Selective Detection of Biological and Chemical Species. *Science*, Vol. 293, pp. 1289-1292, ISSN 0036-8075

[64] Gu, S.Y.; Wang, Z.M.; Li, J.B.; Ren, J. (2010). Switchable Wettability of Thermo-Responsive Biocompatible Nanofibrous Films Created by Electrospinning. *Macromolecular Materials and Engineering*, Vo. 295, pp. 32-36 ISSN 1438-7492.

[65] Adam, D. (2001). Fine Set of Threads, *Nature*, Vol. 411, No. 236, pp. 236-236, ISSN 0028-0836

[66] Yu, J.H.; Sergey, V.F.; Gregory, C.R. (2004). Production of Submicrometer Diameter Fibers by Two-Fluid Electrospinning. *Advanced Materials* Vol. 16, pp. 1562-1566, ISSN 1521-4095.

[67] Dan, L.; Gong, O.; Jesse, T.M.; Younan, X. (2005). Collecting Electrospun Nanofibers with Patterned Electrodes, *Nano Letter*, Vol. 5, pp. 913-916, ISSN 1530-6984.

[68] Donzhi, Y.; Jianfeng, Z.; Jing, Z.; Jun, N. Aligned (2008). Electrospun Nanofibers Induced by Magnetic Field, *Journal of Applied Polymer Science*, Vol. 110, pp. 3368-3372, ISSN 1097-4628.

[69] Bogntizki, M.; Frese, T.; Steinhart, M.; Greiner, A.; Wendoreff, J.H. (2001). Preparation of Fibers with Nanoscaled Morphologies: Electrospinning of Polymer Blends, *Polymer Engineering & Science*, Vol. 41, pp. 982-989, ISSN 1548-2634.

[70] Li, L.; Hsieh, Y. (2005). Ultra-fine Polyelectrolyte Fibers from Electrospinning of Poly(acrylic acid), *Polymer*, Vol. 46, pp. 5133-5139, ISSN 0032-3861.

[71] Chen, H.; Hsieh, Y. (2004). Ultrafine Hydrogel Fibers with Dual Temperatureand pH-Responsive Swelling Behaviors. *Journal of Polymer Science Part A: Polymer Chemistry* ,Vol. 42, pp. 6331-6339, ISSN 1099-0518.

[72] Jin, X.; Hsieh, Y. (2005). pH-Responsive swelling behavior of poly(vinyl alcohol)/poly(acrylic acid) bi-component fibrous hydrogel membranes, *Polymer*, Vol. 46, pp. 5149-5160, ISSN 0032-3861.

[73] Okuzaki, H.; Kobayashi, K.; Yan, H. (2009). Thermo-Responsive Nanofiber Mats, *Macromolecules* Vol. 42, pp. 5916-5918, ISSN 0024-9297.

[74] Jin, X.; Hsieh, Y. Electrospinning (2007). pH-Responsive Block Copolymer Nanofibers. *Advanced Materials*, Vol. 19, pp. 3544-3548, ISSN 1521-4095.

[75] Yoshida, R.; Tanaka, M.; Onodera, S.; Yamaguchi, T.; Kokufuda, E. (2000). In-phase synchronization of chemical and mechanical oscillations in self-oscillating gels, *The Journal of Physical Chemistry A*, Vol. 104, pp. 7549–7555, ISSN 1089-5639.

[76] AK. Horvath, I. Nagypal, G. Peintler, and IR. Epstein (2004). Autocatalysis and self-inhibition: Coupled kinetic phenomena in the chlorite-tetrathionate reaction, *Journal of the American Chemical Society*, vol. 126, No. 20, pp. 6246-6247, ISSN 0002-7863.

[77] J. Boissonade (2005). Self-oscillations in chemoresponsive gels: A theoretical approach, *Chaos*, vol. 15, No. 2, pp. 023703, ISSN 1054-1500.

[78] J. Boissonade (2003) Simple chemomechanical process for self-generation of rhythms and forms, *Physical Review Letters*, Vol. 90, No. 18, pp. 188302, ISSN 0031-9007.

[79] B. G. Kabra, and S. H. Gehrke (1991). Synthesis of fast response, temperature-sensitive poly(N-isopropylacrylamide) gel, *Polymer Communications*, vol. 32, no. 11, pp. 322-323, ISSN 0263-6476.

[80] T. Norisuye, Y. Kida, N. Masui, and Q. Tran-Cong-Miyata (2003). Studies on two types of built-in inhomogeneities for polymer gels: Frozen segmental concentration fluctuations and spatial distribution of cross-links, *Macromolecules*, Vol. 36, No. 16, pp. 6202-6212, ISSN 0024-9297.

[81] A. Onuki (1993). Theory of phase-transition in polymer gels, *Advances in Polymer Science*, Vol. 109, pp. 63-121, ISSN 0065-3195.